Mechanism of autophagy induced by activation of the AMPK/ERK/mTOR signaling pathway after TRIM22-mediated DENV-2 infection of HUVECs

Ning Wu
Guizhou Medical University
Xiaoqin Gou
Guizhou Medical University
Pan Hu
Guizhou Medical University
Yao Chen
Guizhou Medical University
Jinzhong Ji
Guizhou Medical University
Yuanying Wang
Guizhou Medical University
Li Zuo (gzykdxzuoli@163.com)
Guizhou Medical University

Research Article

Keywords: DENV-2, autophagy, AMPK/ERK/mTOR signaling pathway, TRIM22

Posted Date: May 16th, 2022

DOI: https://doi.org/10.21203/rs.3.rs-1648872/v1

Abstract

Background: Dengue virus type 2 (DENV-2) was used to infect primary human umbilical vein endothelial cells (HUVECs) to examine autophagy induced by activation of the adenosine monophosphate-activated protein kinase (AMPK)/extracellular signal-regulated kinase (ERK)/mammalian target of rapamycin (mTOR) signaling pathway following tripartite motif-containing 22 (TRIM22)-mediated DENV-2 infection to further reveal the underlying pathogenic mechanism of DENV-2 infection.

Methods: Quantitative real-time polymerase chain reaction (qRT-PCR) was used to screen putative interference targets of TRIM22 and determine the knockdown efficiency. The effect of TRIM22 knockdown on HUVEC proliferation was determined using the CCK8 assay. Following TRIM22 knockdown, transmission electron microscopy (TEM) was used to determine the ultrastructure of HUVEC autophagosomes and expression of HUVEC autophagy and AMPK pathway-related genes were measured by qRT-PCR. Moreover, HUVEC autophagy and AMPK pathway-related protein expression levels were determined by western blot analysis. Cell cycle and apoptosis were assessed by flow cytometry (FCM) and the autophagosome structure of the HUVECs was observed by TEM.

Results: Western blot results indicated that TRIM22 protein expression levels increased significantly 36 h after DENV-2 infection, which was consistent with the proteomics prediction. The CCK8 assay revealed that HUVEC proliferation was reduced following TRIM22 knockdown ($P < 0.001$). The TEM results indicated that HUVEC autolysosomes increased and autophagy was inhibited after TRIM22 knockdown. The qRT-PCR results revealed that after TRIM22 knockdown, the expression levels of antithymocyte globulin 7 (ATG7), antithymocyte globulin 5 (ATG5), Beclin1, ERK, and mTOR genes decreased ($P < 0.01$); however, the expression of AMPK genes ($P < 0.05$) and P62 genes ($P < 0.001$) increased. FCM revealed that following TRIM22 knockdown, the percentage of HUVECs in the G2 phase increased ($P < 0.001$) along with cell apoptosis. The effect of TRIM22 overexpression on HUVEC autophagy induced by DENV-2 infection and AMPK pathways decreased after adding an autophagy inhibitor.

Conclusions: In HUVECs, TRIM22 protein positively regulates autophagy and may affect autophagy through the AMPK/ERK/mTOR signaling pathway. Autophagy is induced by activation of the AMPK/ERK/mTOR signaling pathway following TRIM22-mediated DENV-2 infection of HUVECs.

Background

Dengue virus (DENV) is a positive-sense, single-stranded RNA virus with a diameter of 50 nm. It is approximately 11 kd long and belongs to the *Flavivirus* genus, Flaviviridae. Humans are generally susceptible to DENV and are a natural DENV host [1]. According to statistics, ~ 3.6 billion people are at risk worldwide [2, 3] and more than 21,000 people die each year. Thus, DENV infection has become a major public health problem of global concern. DENV has four serotypes, i.e., DENV1–4, of which DENV-2 is the most widely transmitted [4]. The main spreading process of DENV is relatively simple. After a female mosquito feeds on the blood of a DENV patient, DENV multiplies in the mosquito body and

spreads to susceptible individuals through mosquito bites [5]. DENV infection causes several self-limiting febrile diseases including dengue fever (DF), dengue hemorrhagic fever (DHF), and dengue shock syndrome (DSS). DHF and DSS are fatal syndromes with clinical manifestations of increased vascular permeability and plasma leakage [6], and further result in multiple organ damage and circulatory system failure, which endangers life [7–9]. Pathogenesis is associated with the dysfunction of vascular endothelial cells and autophagy. Autophagy is activated by DENV infection to prevent the fusion of autophagosomes with lysosomes. DENV replicates, assembles, and matures in autophagosomes, thus evading neutralizing antibodies during transport [10, 11].

Autophagy is a lysosomal-dependent degradation pathway in eukaryotic cells that regulates intracellular homeostasis and affects innate immune mechanisms by modulating pattern-recognition receptors and signal transduction associated with injury-related molecular patterns. Thus, intracellular pathogens (e.g., viruses and bacteria) may be specifically recognized and quickly targeted to the autophagy degradation pathway [12, 13]. Recent studies have shown that DENV-2-induced autophagy exhibits a protective effect on infected cells. Denv-2 activates the autophagy pathway to increase the replication of its RNA, whereas the inhibition of autophagy results in a significant decrease in viral replication [14, 15]. DENV can induce vascular leakage through macrophage migration inhibitor factor secretion and autophagy formation. Infectious autophagy-associated DF vesicles released by DENV-infected cells can protect viral RNA in vesicles and avoid antibody neutralization to promote viral transmission [11]. Previous work indicated that DENV-2 can induce primary human umbilical vein endothelial cells (HUVECs) to induce autophagy through the adenosine monophosphate-activated protein kinase (AMPK)/extracellular signal-regulated kinase (ERK)/mammalian target of rapamycin (mTOR) signaling pathway [16]. However, the mechanism through which DENV-2 activates tuberous sclerosis complex 2 (TSC2) via the AMPK and ERK1/2 pathways causing mTOR inhibition is unclear.

Tripartite motif-containing 22 (TRIM22), also known as Staf50, is an interferon-stimulated gene. Previous studies showed that the TRIM protein family is involved in a wide range of cellular processes, including apoptosis, cell cycle progression, and autophagy [17]. Autophagy is regulated by TRIM22 and has both antiviral and viral replication effects. On the one hand, TRIM22 promotes GEM-induced prosurvival autophagy and protects non-small cell lung cancer (NSCLC) cells from apoptosis [18]. TRIM22 promotes viral replication by regulating autophagy. Related studies have demonstrated that TRIM22 binds with the autophagy-related proteins, unc-51-like autophagy activating kinase 1 (ULK1), and Beclin1 to induce autophagy, thus promoting the replication of the respiratory syncytial virus (RSV) [19]. The preliminary proteomics results of the current study demonstrated that TRIM22 protein expression significantly increased 36 h after HUVECs were infected with DENV-2. A protein–protein interaction analysis in the Search Tool for the Retrieval of Interacting Genes/Proteins (STRING) database revealed that TRIM22 was associated with the AMPK/ERK/mTOR signaling pathway. Therefore, whether TRIM22 is involved in autophagy activation of DENV-2-infected HUVECs through the AMPK/ERK/mTOR pathway remains to be determined. Based on these findings, the mechanism of autophagy induced by the activation of the AMPK/ERK/mTOR signaling pathway following DENV-2 infection was explored. Determining how DENV-2 induces HUVEC autophagy through relevant signal transduction pathways will contribute to the

development of effective immunotherapies and appropriate chemical drugs. In addition, this will provide an important theoretical basis for better understanding the pathogenic mechanism(s) of viral infection and lead to the development of antiviral drugs that target autophagy.

Materials And Methods

Cell strain

The Denv-2 standard strain (NGC strain) was preserved in liquid nitrogen. HUVECs were purchased from ScienCell (Carlsbad, CA, USA). Aedes albopictus cells (C6/36) were purchased from the Kunming Cell Bank of the Chinese Academy of Sciences (Kunming, China). TOP10 competent*Escherichia coli* cells were purchased from the TIANGEN Company (Beijing, China).

Plasmid

Br-v108 vectors (AgeI and EcoRI restriction enzyme cutting sites) were purchased from Shanghai Jikai Gene Technology Co., Ltd. (Shanghai, China). Lv-007 vectors (NheI and AgeI restriction enzyme cutting sites) were purchased from YBR BioSCI Res (Shanghai, China).

Reagents and instruments

Extracellular matrix (ECM) media were purchased from ScienCell. RPMI-1640 media was purchased from Gibco (Thermo Fisher Scientific, Waltham, MA, USA). Trizol was purchased from Sigma-Aldrich (Sigma-Aldrich, Burlington, MA, USA). Hiscript QRT Supermix for quantitative PCR (qPCR) and AceQ qPCR SYBR Green was purchased from Vazyme (Nanjing, China). Antibodies (TRIM22, Beclin1, P62, ATG7, ATG5, mTOR, P-mTOR, AMPK, P-AMPK, ERK, P-ERK, and GAPDH) were purchased from Abcam (Abcam, Cambridge, UK). Age I and EcoRI were purchased from NEB (New England Biolabs, Ipswich, MA, USA). The BCA Protein Assay Kit was purchased from HyClone-Pierce, Inc (Thermo Fisher Scientific). Real-time fluorescence quantitative polymerase chain reaction (PCR) was purchased from ABI (StepOne PLUS, Thermo Fisher Scientific). The gel imager was purchased from Bio-Rad (Bio-Rad, Hercules, CA, USA). The ultraviolet-visible spectrophotometer was purchased from Thermo Fisher Scientific. The chemiluminescence imaging system used was a GE AI600. The microplate reader was purchased from Bio-Rad.

Gene-specific primers

Table 1. Sequence of correlated primers for experiments

Gene	Primer	Length (bp)
P62	F: GCAATGGGCCTGTGGTAG	191
	R: CCCGAAGTGTCCGTGTTT	
ATG7	F: GTTGTTTGCTTCCGTGAC	142
	R: TGCCTCCTTTCTGGTTCT	
ATG5	F: AAGCAACTCTGGATGGGATT	173
	R: GCAGCCACAGGACGAAAC	
TRIM22	F: GAGATGTCTGTGAGCACCAT	136
	R: TCCTTGACCACCTCGTTT	
Beclin1	F: CGTGGAATGGAATGAGAT	110
	R: CGTAAGGAACAAGTCGGTAT	
ERK	F: TGTTCCCAAATGCTGACT	131
	R: GGGTCGTAATACTGCTCC	
AMPK	F: CCGAGAAGCAGAAACACG	167
	R: CACATCAAGGCTCCGAAT	
mTOR	F: GCTGTCATCCCTTTATCG	100
	R: TCTTCTTCTTCTCCCTGTAGTC	
GAPDH	F: TGACTTCAACAGCGACACCCA	121
	R: CACCCTGTTGCTGTAGCCAAA	

Cell culture and identification

HUVECs stored in liquid nitrogen were removed and thawed in a 37 °C water bath. HUVECs were transferred to a T25 cm^2 flask containing 5 mL of ECM complete culture solution (10% FBS, 1% ECGs, and 1% P/S) at 37 °C with 5% CO_2. Cell growth was observed each day after HUVECs had adhered to the wall. The growth density of the HUVECs was 80–90% for subculture. The subculture conditions were 28 °C with 5% CO_2 and ECM complete culture solution was the culture medium. When specific molecules, vWF/Factor VIII and CD31, were identified as positive by immunofluorescence, and HIV-1, HBV, HCV, mycoplasma, bacteria, yeast, and fungi were identified as negative, the first generation was cryopreserved when the number of cells was greater than 5×10^5/mL. In this laboratory, subculture was continued to the fourth generation for the experiments.

DENV-2 virulence test

Aedes albopictus cells (C6/36) were recovered, cultured, and subcultured. At the logarithmic growth stage (density, 80%–90%), the cells were seeded into 96-well plates and cultured at 28 °C in a 5% CO_2atmosphere overnight. HUVECs stored in liquid nitrogen were removed and quickly thawed in a 37 °C water bath. The virus stock was diluted tenfold with an RPMI-1640 maintenance solution. Eight concentrations (10^{-3}–10^{-10}) and eight wells for each concentration were noted. The blank control was established and different dilutions of disease venom were simultaneously added and incubated at 37 °C with 5% CO_2 for 2 h. The supernatant was discarded, the cells were washed with Hank's solution, and a fresh medium (200 μL/well) was added. The culture was continued and cytopathic conditions were observed and recorded. The number of lesion holes at each dilution level was recorded and counted within 5 days and the Reed–Muench method was used to calculate the toxicity of DENV-2 to C6/36.

DENV-2 infects HUVECs

HUVECs were recovered, cultured, and subcultured. The cells were seeded into six-well plates and cultured at 37 °C with 5% CO_2overnight at the logarithmic growth stage (density, 80–90%). DENV-2 was stored in liquid nitrogen, removed, and quickly thawed in a 37 °C water bath. The original virus solution was diluted 10^3, 10^4, and 10^5 times with maintenance solution, and the blank control was established. The diluted disease venom was added and incubated at 37 °C with 5% CO_2 for 2 h. The flask was shaken every 30 min to evenly distribute the venom. The supernatant was discarded and the cells were washed twice with Hank's wash solution. A maintenance solution was added and the culture was continued for 36 h. Total protein from cells in the experimental and blank groups was collected.

TEM detection of HUVEC autophagosomes

HUVECs were infected with DENV-2 virus stock solution, which was diluted 10^5 times. Simultaneously, the blank control was set at 37 °C with 5% CO_2 and the cells were collected at 24 and 36 h. The cells were analyzed by electron microscopy at the Chongqing Medical University after fixing with 2.5% glutaraldehyde. The ultrastructure of the cells was observed by TEM and imaged after dehydration, resin soaking, embedding, sectioning, and staining.

TRIM22 gene RNA interference interferes with plasmid vector construction

Using the *TRIM22* gene as a template, three RNA interference target sequences were designed and an RNA interference lentiviral vector was constructed. shTRIM22-1, shTRIM22-2, and shTRIM22-3 represent the knockdown shRNA targets at three different sites designed for the *TRIM22* gene. shRNA interference sequences were designed following the selected target sequences, and appropriate restriction enzyme sites were included at both ends. A double-stranded DNA oligo was prepared and linearized by Age I and EcoR I double digestion of the BR-V108 vector, ligated into the linearized vector, and transformed into TOP10-competent*E. coli* cells by heat shock. After screening, monoclonal expansion culture was conducted, the bacterial fluid was collected, and the plasmid was isolated using the Zyokang GTC endotoxin-free plasmid extraction kit. The plasmid concentration was measured using a

microspectrophotometer. The plasmid was identified by 1% agarose gel electrophoresis after PCR amplification.

Construction of a *TRIM22* gene-overexpressing lentiviral vector

The lV-007 vector was linearized by Nhe I and Age I double digestion. The target gene fragment was amplified by PCR. The homologous recombination sequence was added to the 5' end of the amplimer, and the 5'- and 3'-terminal sequences of the amplified product matched that of the linearized clone vector. The linearized vector and the target gene fragment were recombined *in vitro*. The recombinant plasmid was transformed into the recipient cell, and individual clones were selected for identification by PCR and DNA sequencing. The positive clones were expanded and extracted to obtain plasmid with high purity.

Lentivirus infection of HUVECs

HUVECs in the logarithmic phase (cell density reaching 80%–90%) were divided into an shCtrl group (lentivirus empty vector transfection group, as negative control, NC control group) and an shTRIM22 group (TRIM22 knockdown group). The cells (1×10^5) were inoculated cells into six-well plates and supplemented with EMC complete culture medium to 2 mL. The plates were mixed and incubated at 37 °C with 5% CO_2 for 24 h. The supernatants were discarded and 1 mL of opti-MEM serum-free medium was added to each well. NC control virus and TRIM22 knockdown virus were added at 10^8 $TCID_{50}$/mL, shaken, and incubated at 37 °C with 5% CO_2 for 18 h. The supernatant was discarded and 2 mL of ECM complete culture medium was added to each well for 48 h. The fluorescence intensity and infection efficiency were assessed by fluorescence microscopy.

Quantitative real-time PCR detection

Total RNA was extracted using Trizol from the NC control virus infected with DENV-2 and HUVECs treated with TRIM22 knockdown virus during the logarithmic growth period. The concentration and purity of RNA were measured using an ultramicro-ultraviolet-visible spectrophotometer, and cDNA was obtained by reverse transcription using the RNA as a template. The expression of the target genes was measured by SYBR Green-based qPCR. The procedure was as follows: predenaturation at 95 °C for 1 min, denaturation at 95 °C for 10 s, annealing at 60 °C for 30 s, and repetition of this program for 40 cycles. A melt curve was also established for each gene. Relative quantitative analysis $F = 2^{-\triangle\triangle Ct}$ was used, where $\triangle Ct$ represents the Ct value of the target gene minus the Ct value of the reference gene, $-\triangle\triangle Ct$ is the average value of $\triangle Ct$ in the group C– $\triangle Ct$ value of each sample. In addition, $2^{-\triangle\triangle Ct}$ reflects the relative expression level of target genes in each sample compared with the NC group. GAPDH expression was used as an internal reference.

Cell cycle assay

HUVECs in the logarithmic growth stage were counted and the cells were seeded into six-well plates and cultured with NC control virus and TRIM22 knockdown virus at 10^8 $TCID_{50}$/mL. After the cells of the

HUVEC NC and TRIM22 knockdown groups reached 90%, 300 μL of ECM medium was added to each well to prepare a cell suspension. The cells were collected in 5-mL centrifuge tubes with three wells per group. After centrifugation at 1,300 rpm for 5 min, the supernatant was discarded and the propidium iodide staining solution was added to resuspend the cells. The cells were analyzed by flow cytometry (FCM) after incubating in the dark for 20 min.

CCK8 assay for cell proliferation

HUVECs were seeded into six-well plates and cultured with NC control and TRIM22 knockdown viruses at 10^8 $TCID_{50}$/mL. After cell fusion, the HUVEC NC and TRIM22 knockdown groups were cultured to a density of 90% and counted. The NC and TRIM22 knockdown groups were then inoculated into 96-well plates at 5×10^3 cells/100 μL with three wells for each group. Next, 10 μL of CCK8 solution was added to each well, mixed, and incubated at 37 °C with 5% CO_2 for 4 h. The absorbance at 450 nm was measured with a microplate reader and the experimental data were recorded.

Cell apoptosis

HUVECs were seeded into six-well plates and cultured with NC control and TRIM22 knockdown viruses at 10^8 $TCID_{50}$/mL. After the cells reached 90% confluence, the cell suspensions were collected, centrifuged at 1,300 rpm for 3 min, and resuspended with 1 mL of 1× binding buffer. Then, 5 μL of Annexin V-APC dye was added to each tube and mixed gently, followed by the addition of 10 μL of PI dye. The cells were analyzed within 1 h by FCM after incubating for 20 min on ice at room temperature without light.

Western blot analysis

Cells in the logarithmic phase were collected from each group and washed twice with Hank's solution. The residual solution was discarded, and the cells were lysed in RIPA buffer (PMSF:RIPA = 1:100) containing protease and phosphoprotease inhibitors. The cells were shaken and lysed on ice, scraped off at 4 °C, and centrifuged at 12,000 rpm for 30 min. The supernatant was transferred to 1.5-mL centrifuge tubes and the concentration of each protein sample was measured by the BCA method. A 5× protein loading buffer was added to 40 μg of total protein for each sample. The proteins were separated by sodium dodecyl sulfate–polyacrylamide gel electrophoresis at 80 V for 20 min followed by 120 V for 100 min. Following the transfer, the PVDF membranes were blocked with 5% skim milk for 120 min and incubated with primary antibody overnight. TBST was used to wash the membranes six times for 5 min each. The secondary antibody was added and incubated at room temperature for 120 min on a shaking table. After chemiluminescent detection, Image J software was used to analyze the relative amount of each protein band.

Statistical analysis

The experimental data were analyzed by Statistical Product and Service Solutions 25.0 (SPSS25.0). All experiments were repeated at least three times. The data were plotted using GraphPad Prism 8.0

software. The data that conformed to a normal distribution were expressed as the mean ± standard deviation (±s). One-way analysis of variance was used for comparisons between groups, and a Student's *t*-test was used for pairwise comparison. $P < 0.05$ was considered statistically significant.

Results

TRIM22 protein expression increases in HUVECs after DENV-2 infection

DENV-2 at a concentration of 10^5 $TCID_{50}$/mL was used to infect HUVECs for 36 h. The expression of HUVEC TRIM22 protein was determined by western blot analysis. Compared with the control group, TRIM22 protein expression in the DENV-2-infected group significantly increased ($P < 0.001$).

qRT-PCR analysis of interference targets of TRIM22

The qRT-PCR results indicated that compared with the shCtrl group, the *TRIM22* gene knockdown efficiency in the shTRIM22-1, SHTRIM22-2, and SHTRIM22-3 groups were 30.6% ($P < 0.05$), 52.5% ($P < 0.01$), and 98.1% ($P < 0.01$), respectively. Therefore, the shTRIM22-3 group was used to conduct subsequent experiments.

Knockdown efficiency detection

The qRT-PCR results indicated that, compared with the shCtrl group, the knockdown efficiency of shTRIM22 on HUVECs was 90.43% ($P < 0.05$). Western blot analysis confirmed that, compared with the shCtrl group, the expression of TRIM22 protein in the shTRIM22 group significantly decreased ($P < 0.001$), indicating that TRIM22 knockdown was successful.

Lentivirus infects HUVECs

Significant green fluorescence was observed by microscopy after a 72-h infection of HUVECs with lentivirus in the shCtrl or shTRIM22 groups. The results indicated that the infection efficiency was >80% and the cell morphology was normal.

Effect of shTRIM22 on cell proliferation

The *TRIM22* gene was used to construct a TRIM22 knockdown lentivirus vector, which was transfected into HUVECs. The CCK8 method was used to assess changes in cell viability over five consecutive days. The cell proliferation results are shown in Figure 5. After lentivirus infection, compared with the shCtrl group, the OD value of the shTRIM22 group was smaller at the same time point, indicating that the proliferation rate of the HUVECs in the shTRIM22 group was slower. The difference was statistically significant ($P < 0.001$), indicating that TRIM22 affects HUVEC proliferation.

Ultrastructure of HUVEC autophagosomes after TRIM22 knockdown using TEM

Figure 6 shows scattered vacuoles observed in both the shCtrl and shTRIM22 groups, which were surrounded by a membrane. The nuclear fragments and organelles were evident in the small body. However, compared with the shCtrl group, the ultrastructure of HUVEC autophagosomes following TRIM22 knockdown showed increased autophagolysosomes and reduced autophagy, indicating that TRIM22 knockdown significantly affects autophagy in HUVECs.

TRIM22 knockdown affects the expression of HUVEC autophagy and AMPK pathway-related genes

The qRT-PCR results indicated that, compared with the shCtrl group, the expression of ATG7, ATG5, Beclin1, ERK, and mTOR genes in HUVECs with TRIM22 knockdown ($P < 0.01$) as well as the expression of *TRIM22* genes ($P < 0.001$) were downregulated. In contrast, the mRNA expression of *AMPK* ($P < 0.05$) and *P62* ($P < 0.001$) genes was upregulated. These results indicate that TRIM22 upregulates the expression of autophagy and AMPK signaling pathway-related genes in HUVECs.

TRIM22 knockdown affects the expression of autophagy-related proteins in HUVECs

Compared with the shCtrl group, the expression of ATG5, ATG7, Beclin1, and LC3B-II protein in HUVECs with TRIM22 knockdown decreased ($P < 0.001$), whereas P62 protein expression was increased ($P < 0.01$). This indicates that autophagy was inhibited following TRIM22 knockdown and shows that TRIM22 induces autophagy.

TRIM22 knockdown affects the expression of AMPK pathway-related proteins

Compared with the shCtrl group, the expression of p-AMPK and p-ERK decreased in HUVECs with TRIM22 knockdown ($P < 0.001$), whereas p-mTOR expression increased ($P < 0.01$), indicating that TRIM22 may have a positive regulatory effect on the AMPK/ERK/mTOR pathway.

Effect of TRIM22 knockdown on the cell cycle

Intracellular DNA content was stained with PI and subjected to FCM for cell cycle analysis. Figure 10 shows that the proportion of HUVECs in the G1/G0 phase decreased ($P < 0.05$) and that in the S phase decreased ($P < 0.05$) compared with the shCtrl group 36 h after DENV-2 treatment of HUVECs with TRIM22 knockdown. An increased cell number in the G2/M phase was also observed (28.53%/34.36%, $P < 0.001$). TRIM22 knockdown blocked the DNA synthesis phase (S phase) and promoted the late DNA synthesis phase (G2/M phase).

Effect of TRIM22 knockdown on apoptosis in HUVECs infected with DENV-2

FCM was used to determine the effect of TRIM22 knockdown on apoptosis in HUVECs infected with DENV-2 (Figure 11). The results indicated that the total apoptosis rate of the shCtrl group was 4.59% (early apoptosis, 3.18%; late apoptosis, 1.41%) and that of DENV-2 + shCtrl group was 10.07% (early apoptosis, 5.42%; late apoptosis, 4.65%). The total apoptosis rate of the DENV-2 + shTRIM22 group was 40.86% (early stage, 31.39%; late stage, 9.47%). This suggests that HUVECs with TRIM22 knockdown

contain more early apoptotic cells (LR) and late apoptotic cells (UR) compared with the control group. The total apoptosis rate (UR + LR) of the HUVECs with TRIM22 knockdown was also significantly higher compared with the control group ($P < 0.001$). These results indicated that TRIM22 knockdown promotes apoptosis of HUVECs infected with DENV-2.

Autophagy ultrastructure of DENV-2-infected HUVECs with TRIM22 knockdown using TEM

TEM results showing the ultrastructural morphology of HUVECs are shown in Figure 12. Scattered vacuoles surrounded by a membrane in each group of cells were noted, and nuclear fragments and organelles were observed in small bodies. Compared with the shCtrl group, HUVEC autolysosomes increased after TRIM22 knockdown. The results indicate that autophagy of HUVECs was inhibited following TRIM22 knockdown.

Effects of TRIM22 knockdown on DENV-2-induced autophagy and AMPK pathway-related protein expression

Whether the regulatory effect of TRIM22 on HUVEC autophagy occurs during DENV-2 infection was further explored. Thus, negative control (shCtrl), TRIM22 knockdown (shTRIM22), AMPK activator (AICAR), and TRIM22 knockdown + AMPK activator (shTRIM22 + AICAR) groups were established. All groups were infected with DENV-2 for 36 h, except for the negative control group. Western blot analysis was used to determine the effects of TRIM22 knockdown on the expression of autophagy proteins ATG1, ATG5, ATG7, Beclin1, and P62 and the activation of AMPK, ERK, and mTOR proteins of the AMPK/ERK/mTOR pathway in HUVECs. The results indicated that TRIM22 induced autophagy in HUVECs following DENV-2 infection. TRIM22 knockdown during DENV-2 infection reduced autophagy in HUVECs. These results suggest that TRIM22 promotes autophagy in HUVECs following DENV-2 infection, whereas TRIM22 knockdown reduces the induction of autophagy through the AMPK/ERK/mTOR signaling pathway.

Effect of TRIM22 knockdown on DENV-2-induced HUVEC autophagy

Compared with the shCtrl group, the shTRIM22 group exhibited reduced expression of ATG1 ($P < 0.01$), ATG5 ($P < 0.05$), ATG7 ($P < 0.001$), and Beclin1 ($P < 0.01$) following DENV-2 infection of HUVECs with TRIM22 knockdown, whereas P62 expression levels increased ($P < 0.05$). These results suggest that TRIM22 knockdown has an inhibitory effect on DENV-2-induced autophagy. In the AICAR group, ATG1 ($P < 0.05$), ATG5 ($P < 0.01$), ATG7 ($P < 0.001$), and Beclin1 ($P < 0.001$) expression increased, whereas P62 expression decreased ($P < 0.01$). These results indicate that the expression of autophagy proteins following DENV-2-infection of HUVECs was enhanced following stimulation with an AMPK activator.

In the shTRIM22 + AICAR group, compared with the shTRIM22 group, the expression levels of ATG1 ($P < 0.05$), ATG5 ($P < 0.01$), ATG7 ($P < 0.001$), Beclin1 ($P < 0.001$), and LC3II/LC3I ($P < 0.05$) increased, whereas P62 expression levels decreased ($P < 0.01$). Compared with the AICAR group, in the shTRIM22 + AICAR group, the expression levels of ATG1 ($P < 0.01$), ATG5 ($P < 0.05$), ATG7 ($P < 0.001$), Beclin1 ($P <$

0.001), and LC3II/LC3I ($P < 0.001$) decreased, whereas the P62 expression levels increased ($P < 0.05$). These results suggest that TRIM22 knockdown reduces autophagy induced by DENV-2 infection combined with an AMPK activator in HUVECs.

Effect of TRIM22 knockdown on AMPK pathway-related proteins in DENV-2-infected HUVECs

Compared with the shCtrl group, following DENV-2 infection of HUVECs with TRIM22 knockdown, the expression of p-AMPK and p-ERK in the shTRIM22 group decreased ($P < 0.01$), whereas p-mTOR expression increased ($P < 0.05$). This indicates that TRIM22 knockdown downregulates the AMPK/ERK/mTOR signaling pathway. In the AICAR group, the expression of p-AMPK and p-ERK protein increased ($P < 0.001$), whereas p-mTOR protein expression decreased ($P < 0.001$). This suggests that AMPK/ERK/mTOR signaling is upregulated following stimulation with an AMPK activator.

Compared with the AICAR group, the expression of p-AMPK and p-ERK in the shTRIM22 + AICAR group decreased ($P < 0.01$) and p-mTOR expression increased ($P < 0.05$). Compared with the shTRIM22 group, the expression of p-AMPK and p-ERK in the shTRIM22 + AICAR group increased ($P < 0.001$), whereas p-mTOR protein expression decreased ($P < 0.01$). These results suggest that TRIM22 knockdown inhibits the activity of the AMPK/ERK/mTOR pathway induced by DENV-2 infection combined with an AMPK activator.

Effects of TRIM22 overexpression on DENV-2-infected HUVEC autophagy and AMPK pathway-related proteins

The Empty vector, TRIM22-OE, Dorsomorphin, and TRIM22-OE + Dorsomorphin groups were established to confirm the regulatory effect of TRIM22 on autophagy. All groups were infected with DENV-2 for 36 h, except for the shCtrl group. Western blot analysis was used to detect the HUVEC autophagy and the expression of AMPK pathway-related proteins. The results showed that TRIM22 promotes HUVEC autophagy induced by DENV-2 infection through positive regulation of the AMPK/ERK/mTOR signaling pathway.

Establishment of a TRIM22 overexpression plasmid

The vector map of a TRIM22 overexpression plasmid is shown in Figure 15B. The linearized vector was obtained by Nhe I and Age I digestion, and the target gene fragment (Figure 15A) was obtained by PCR amplification (Figure 15C). The homologous recombination sequence was added to the 5'-end of the amplicon, and the 5'- and 3'-terminal sequences of the amplified product matched the linearized clone vector. The linearized vector and target gene fragment were recombined *in vitro* and transformed in *E. coli*. PCR product identification was done (Figure 15D), and the results of positive clone sequencing were identical to the expected target sequence (see Appendix).

Detection of TRIM22 overexpression efficiency

RT-qPCR results showed that compared with the empty vector group, the TRIM22 mRNA expression level in the TRIM22-OE group significantly increased (P<0.01).

Effect of TRIM22 overexpression on autophagy-related proteins following DENV-2-infection of HUVECs

Compared with the Empty vector group, after DENV-2 infection of TRIM22-overexpressing HUVECs, the expression of ATG5 in the TRIM22-OE group increased (P < 0.01); the expression levels of ATG7, Beclin1, and LC3B-II increased (P < 0.001); and the expression of P62 decreased (P < 0.001). The expression of ATG5 (P < 0.05), ATG7 (P < 0.001), Beclin1 (P < 0.01), and LC3II/LC3I (P < 0.05) in the Dorsomorphin group decreased, whereas the P62 expression levels increased (P < 0.01). This indicates that AMPK inhibitors inhibit autophagy.

Compared with the TRIM22-OE group, the expression of ATG5 (P < 0.05), ATG7 (P<0.01), Beclin1 (P < 0.01), and LC3II/LC3I (P < 0.01) in the TRIM22-OE + Dorsomorphin group decreased, whereas P62 expression levels increased (P < 0.05). Compared with the Dorsomorphin group, the expression of ATG5 (P < 0.01), ATG7 (P < 0.001), Beclin1 (P < 0.001), and LC3II/LC3I (P < 0.001) in the TRIM22-OE + 3-MA group increased, whereas P62 expression levels decreased (P < 0.01). These results indicate that TRIM22 reduces the inhibitory effects of AMPK inhibitors on autophagy, suggesting that TRIM22 promotes autophagy induced by DENV-2 infection.

Effect of TRIM22 overexpression on AMPK-related proteins in DENV-2-infected HUVECs

Compared with the Empty vector group, after DENV-2 infection of HUVECs with TRIM22 overexpression, the expression of p-AMPK (P < 0.001) and p-ERK (P < 0.001) in the TRIM22-OE group increased, whereas p-mTOR expression levels decreased (P < 0.01). These results indicate that TRIM22 activates the AMPK/ERK/mTOR pathway. In the Dorsomorphin group, the expression levels of p-AMPK (P < 0.001) and p-ERK (P < 0.001) decreased, whereas p-mTOR expression levels increased (P < 0.01). These results indicated that Dorsomorphin inhibits the expression of the AMPK/ERK/mTOR pathway.

Compared with the TRIM22-OE group, the expression of p-AMPK (P < 0.01) and p-ERK (P < 0.01) in the TRIM22-OE + Dorsomorphin group was downregulated, whereas the p-mTOR protein expression levels were upregulated (P < 0.01). Compared with the Dorsomorphin group, the expression of p-AMPK (P < 0.001) and p-ERK (P < 0.001) in the TRIM22-OE + Dorsomorphin group was upregulated, whereas p-mTOR expression levels were downregulated (P < 0.01). These results indicate that TRIM22 overexpression reduces the inhibitory effect of AMPK inhibitors on the AMPK/ERK/mTOR pathway, suggesting that TRIM22 enhances DENV-2 infection-induced autophagy through the AMPK/ERK/mTOR signaling pathway.

Discussion

In recent years, studies have suggested that DENV induces autophagy to prevent host cell death and enhance viral replication. Activation of autophagy regulates lipid metabolism and provides materials and

energy for DENV replication, whereas inhibition of autophagy results in a significant decrease in viral replication [14, 15]. Previous studies showed that DENV-2-infected HUVECs induced autophagy through the AMPK/ERK/mTOR signaling pathway; however, which host cell molecules are activated by DENV-2 to regulate AMPK and ERK1/2 signaling is unclear. Therefore, the mechanism of DENV-2 activation of the AMPK/ERK/mTOR signaling pathway was examined to induce autophagy at the host protein level.

TRIM22 belongs to the TRIM protein family, which contains ~ 80 members. It is characterized as an N-terminal RING domain, one or two B-box domains, and a curly helix domain. Of these, the RING domain exhibits E3 ubiquitin ligase activity, whereas the B-box and curly helix domain mediate protein–protein interactions [20]. Members of the TRIM family are involved in various biological processes including cell cycle regulation, autophagy, antiviral immunity, tumorigenesis, and tumor progression [21]. TRIM22 expression may be induced by interferon and its 5' flanking region gene contains two homologous sequences of IFN-stimulated response elements, which bind to IFN regulatory factor 1 in response to types I and II IFN stimulation and induce TRIM22 expression [22]. In addition to interferon, TRIM22 expression is also regulated by viruses and viral antigens [23]. As a member of the TRIM family, TRIM22 regulates viral infection through various mechanisms. Since its discovery, TRIM22 is characterized by its ability to inhibit HIV-1 transcription. TRIM22 inhibits basic HIV-1 transcription by preventing Sp1 from binding to the HIV-1 promoter, thus inhibiting HIV-1 infection [24]. The binding of TRIM22 to the influenza virus nuclear protein promotes its downregulation through ubiquitination degradation and plasmosome dependence to inhibit influenza virus replication [25]. TRIM22 also inhibits herpes simplex viruses by promoting chromatin compression to silence viral DNA encoding early viral genes [26]. TRIM22 also inhibits hepatitis B virus and gamma herpesvirus [27]. Recent studies showed that the TRIM protein family is also involved in DENV infection. TRIM69 degrades Lys104 amino acid residues of DENV NS3 by ubiquitinating its RING domain through E3 ubiquitin ligase activity to inhibit DENV replication [28]. The subgenomic RNA of DENV-2 inhibits RIG-I activation and IFN expression by binding to TRIM25 [29].

Autophagy is a highly conserved intracellular catabolic process and abnormal autophagy is closely associated with the occurrence and development of various diseases [30]. Several studies have demonstrated that TRIM family members can regulate autophagy through various pathways, including the regulation of autophagy-related signaling pathways and autophagy core molecules as autophagy substrate recognition receptors [31]. Related studies have indicated that TRIM5α promotes the initiation of autophagy by promoting the interaction between activated ULK1 and Beclin1 [32]. TRIM39 knockdown enhances the accumulation of autophagosomes and promotes autophagic flux in a Rab7-dependent manner [33]. TRIM65 knockdown inhibits autophagy of A549/DDP cells through the miR-138-5P/ATG7 pathway [34], whereas TRIM14 promotes autophagy in gastric cancer cells by activating the AMPK pathway [35].

Autophagy plays a dual role in viral infection. It inhibits viral replication and can also be exploited by the virus to promote its replication [36]. Viruses that are cleared by autophagy include herpes simplex virus type I, sindbis virus, and human immunodeficiency virus type I. Viruses that utilize autophagy to promote their replication include Coxsackie virus B3, hepatitis C virus, and Zika virus [34, 36]. Similarly, DENV

induces autophagy to prevent host cell death and enhance its viral replication. In addition, activation of autophagy regulates lipid metabolism and provides the energy and materials for DENV replication, while inhibition of autophagy leads to a significant decrease in viral replication [11, 14]. During viral infection, the TRIM family regulates virus–host cell interactions by regulating autophagy. Several mechanisms involving TRIM proteins in virus-induced autophagy have been reported. Some TRIM proteins act as specific substrate receptors that directly recognize viral components, which they target to mediate autophagic degradation. Some TRIM proteins regulate the activity of key signaling proteins involved in various steps of the autophagy pathway [37]. TRIM5α not only directly recognizes the HIV capsid protein to mediate its autophagic degradation but also promotes the degradation of the HIV capsid protein by regulating autophagy-related molecules [38]. TRIM16 promotes antiviral autophagy by promoting the activation of the P62-NRF2 axis [39]. TRIM23 mediates virus-induced autophagy by activating TANK-bound kinase 1 (TBK1) [40]. Similar studies indicate that TRIM22 can also regulate autophagy. TRIM22 regulates macrophage autophagy through NF-κB/Beclin1 signaling [17], promotes GEM-induced prosurvival autophagy, and protects NSCLC cells from apoptosis [18]. TRIM22, however, promotes viral replication by regulating autophagy. Related studies have shown that TRIM22 binds to the autophagy-related proteins, ULK1 and Beclin1, to induce autophagy, thus promoting RSV replication [19].

Based on the above findings and previous proteomics results, the current study hypothesized that TRIM22 may be involved in the autophagic regulation of HUVECs infected with DENV-2. The present study first determined the virulence of DENV-2 and the optimal concentration required to induce HUVEC autophagy. TRIM22 expression was increased in DENV-2-infected HUVECs, confirming the previous proteomic results. TRIM22 was also knocked down in HUVECs causing the proliferation rate to decrease, the expression of autophagy-related proteins to decrease, and autolysosomes to increase. This suggests that TRIM22 knockdown inhibits autophagy, which is consistent with previous reports that TRIM22 promotes autophagy. Moreover, following TRIM22 knockdown, protein phosphorylation levels of AMPK and ERK decreased, whereas that of mTOR increased. These results suggest that TRIM22 activates autophagy through the AMPK/ERK/mTOR signaling pathway. TRIM22 induces autophagy in HUVECs through the AMPK/ERK/mTOR signaling pathway.

To determine whether TRIM22 plays a role in regulating autophagy following DENV-2 infection of HUVECs, the current study examined DENV-2-infected HUVECs with TRIM22 knockdown. HUVECs in the G2 phase of the cell cycle increased, apoptosis increased, autophagy-related protein levels decreased, and the number of autolysosomes increased. This indicates that an effect on TRIM22 on HUVEC autophagy occurs during DENV-2 infection. Moreover, TRIM22 knockdown during DENV-2 infection ameliorates the activation effect of an autophagy activator on HUVEC autophagy. These results suggest that TRIM22 promotes autophagy induced by HUVECs infected with DENV-2. Autophagy and apoptosis control intracellular homeostasis. In general, autophagy blocks the induction of apoptosis, enabling cells to adapt to environmental stress. Both processes are under the control of multiple common upstream signals, and cross-regulation exists between them as a form of inhibition [41]. Therefore, TRIM22 knockdown results in increased HUVECs in the G2 phase of the cell cycle and increased apoptosis may be caused by autophagy inhibition. To confirm the regulation of TRIM22 on autophagy, TRIM22 was

overexpressed in HUVECs and infected with DENV-2. The results indicated that autophagy increased and TRIM22 overexpression reduced the inhibitory effect of autophagy inhibitors on autophagy. The increased expression of TRIM22 during DENV-2 infection was confirmed to promote HUVEC autophagy. TRIM22 was knocked down and overexpressed in HUVECs followed by infection with DENV-2 to further explore whether TRIM22 mediates DENV-2-induced autophagy through the AMPK/ERK/mTOR pathway. Following TRIM22 knockdown, protein phosphorylation levels of AMPK and ERK decreased, whereas that of mTOR increased. In addition, the positive regulatory effect of an autophagy activator on the AMPK/ERK/mTOR pathway decreased by TRIM22 knockdown. In contrast, activation of the AMPK/ERK/mTOR pathway increased after TRIM22 overexpression, and the negative regulatory effect of autophagy inhibitors on the AMPK/ERK/mTOR pathway was reduced as a result of TRIM22 overexpression. This indicates that TRIM22 is involved in the autophagy activation of DENV-2-infected HUVECs through the AMPK/ERK/mTOR pathway.

This study confirmed, for the first time, that TRIM22 is involved in DENV-2-induced autophagy through the AMPK/ERK/mTOR signaling pathway; however, the details of this regulatory mechanism remain to be defined. Future studies will explore the mechanism through which DENV-2 promotes TRIM22 expression and the relationship between TRIM22 and the AMPK pathway to better understand the mechanism of DENV-2-induced autophagy.

Abbreviations

DENV-2: dengue virus type 2

HUVECs: primary human umbilical vein endothelial cells

AMPK: adenosine monophosphate-activated protein kinase

ERK: extracellular signal-regulated kinase

mTOR: mammalian target of rapamycin

TRIM22: tripartite motif-containing 22

qRT-PCR: quantitative real-time polymerase chain reaction

TEM: transmission electron microscopy

FCM: flow cytometry

ATG7: antithymocyte globulin 7

ATG5: antithymocyte globulin 5

DENV: dengue virus

DF: dengue fever

DHF: dengue hemorrhagic fever

DSS: dengue shock syndrome

TSC2: tuberous sclerosis complex 2

NSCLC: non-small cell lung cancer

ULK1: unc-51-like autophagy activating kinase 1

RSV: respiratory syncytial virus

STRING: Search Tool for the Retrieval of Interacting Genes/Proteins

ECM: extracellular matrix

PCR: polymerase chain reaction

LR: early apoptotic cell

UR: late apoptotic cell

OE: overexpression group

AICAR: 5-aminoimidazole-4-carboxamide 1-β-D-ribofuranoside

TBK1: TANK-bound kinase 1

Declarations

Ethics approval and consent to participate

Not applicable.

Consent for publication

Not applicable.

Availability of data and materials

The datasets used and/or analysed during the current study are available from the corresponding author on reasonable request.

Competing interests

The authors declare that they have no competing interests.

Funding

This work was supported by the National Natural Science Foundation of China (81860289) and National College Students Innovation and Entrepreneurship Training Program, China (20195200146).

Authors' contributions

NW participated in conceptualization, design, data curation, formal analysis, investigation, methodology, writing-original draft, statistical analysis, writing-review & editing. XG and PH design the study, wrote the manuscript, and performed the experiments. YC, JJ, and YW performed the experiments, conducted formal analysis, and assisted with the statistical analysis. LZ contributed to conceptualization, methodology, validation, statistical analysis, resources, writing-review & editing, supervision, project administration, and funding acquisition. All authors read and approved the final manuscript.

Acknowledgements

The authors thank all members from the Department of Immunology and the Chemistry and Biochemistry Laboratory for their help and support in all aspects of this work.

References

1. Roy SK, Bhattacharjee S: **Dengue virus: epidemiology, biology, and disease aetiology**. Can J Microbiol 2021, **67**:687–702.
2. Yenamandra SP, Koo C, Chiang S, Lim HSJ, Yeo ZY, Ng LC, Hapuarachchi HC: **Evolution, heterogeneity and global dispersal of cosmopolitan genotype of Dengue virus type 2**. Sci Rep 2021, **11**:13496.
3. Stanaway JD, Shepard DS, Undurraga EA, Halasa YA, Coffeng LE, Brady OJ, Hay SI, Bedi N, Bensenor IM, Castañeda-Orjuela CA, et al: **The global burden of dengue: an analysis from the Global Burden of Disease Study 2013**. Lancet Infect Dis 2016, **16**:712–723.
4. Mustafa MS, Rasotgi V, Jain S, Gupta V: **Discovery of fifth serotype of dengue virus (DENV-5): A new public health dilemma in dengue control**. Med J Armed Forces India 2015, **71**:67–70.
5. Colpitts TM, Cox J, Vanlandingham DL, Feitosa FM, Cheng G, Kurscheid S, Wang P, Krishnan MN, Higgs S, Fikrig E: **Alterations in the Aedes aegypti transcriptome during infection with West Nile, dengue and yellow fever viruses**. PLoS Pathog 2011, **7**:e1002189.
6. Nanaware N, Banerjee A, Mullick Bagchi S, Bagchi P, Mukherjee A: **Dengue Virus Infection: A Tale of Viral Exploitations and Host Responses**. Viruses 2021, **13**.
7. St John AL, Abraham SN, Gubler DJ: **Barriers to preclinical investigations of anti-dengue immunity and dengue pathogenesis**. Nat Rev Microbiol 2013, **11**:420–426.
8. Herrero LJ, Zakhary A, Gahan ME, Nelson MA, Herring BL, Hapel AJ, Keller PA, Obeysekera M, Chen W, Sheng KC, et al: **Dengue virus therapeutic intervention strategies based on viral, vector and host**

factors involved in disease pathogenesis. Pharmacol Ther 2013, **137**:266–282.

9. Jácome FC, Caldas GC, Rasinhas ADC, de Almeida ALT, de Souza DDC, Paulino AC, da Silva MAN, Bandeira DM, Barth OM, Dos Santos FB, Barreto-Vieira DF: **Immunocompetent Mice Infected by Two Lineages of Dengue Virus Type 2: Observations on the Pathology of the Lung, Heart and Skeletal Muscle**. Microorganisms 2021, **9**.
10. Nasar S, Rashid N, Iftikhar S: **Dengue proteins with their role in pathogenesis, and strategies for developing an effective anti-dengue treatment: A review**. J Med Virol 2020, **92**:941–955.
11. Wu SY, Chen YL, Lee YR, Lin CF, Lan SH, Lan KY, Chu ML, Lin PW, Yang ZL, Chen YH, et al: **The Autophagosomes Containing Dengue Virus Proteins and Full-Length Genomic RNA Are Infectious**. Viruses 2021, **13**.
12. Kitada M, Koya D: **Autophagy in metabolic disease and ageing**. Nat Rev Endocrinol 2021, **17**:647–661.
13. Hill SM, Wrobel L, Rubinsztein DC: **Post-translational modifications of Beclin 1 provide multiple strategies for autophagy regulation**. Cell Death Differ 2019, **26**:617–629.
14. Heaton NS, Randall G: **Dengue virus-induced autophagy regulates lipid metabolism**. Cell Host Microbe 2010, **8**:422–432.
15. Lee YR, Lei HY, Liu MT, Wang JR, Chen SH, Jiang-Shieh YF, Lin YS, Yeh TM, Liu CC, Liu HS: **Autophagic machinery activated by dengue virus enhances virus replication**. Virology 2008, **374**:240–248.
16. Kong W, Mao J, Yang Y, Yuan J, Chen J, Luo Y, Lai T, Zuo L: **Mechanisms of mTOR and Autophagy in Human Endothelial Cell Infected with Dengue Virus-2**. Viral Immunol 2020, **33**:61–70.
17. Lou J, Wang Y, Zheng X, Qiu W: **TRIM22 regulates macrophage autophagy and enhances Mycobacterium tuberculosis clearance by targeting the nuclear factor-multiplicity κB/beclin 1 pathway**. J Cell Biochem 2018, **119**:8971–8980.
18. Wang Y, Liang HX, Zhang CM, Zou M, Zou BB, Wei W, Hu W: **FOXO3/TRIM22 axis abated the antitumor effect of gemcitabine in non-small cell lung cancer via autophagy induction**. Transl Cancer Res 2020, **9**:937–948.
19. Yu ZB: **TRIM22 regulates RSV replication through autophagy**. Hebei Medical University, 2018.
20. Khan R, Khan A, Ali A, Idrees M: **The interplay between viruses and TRIM family proteins**. Rev Med Virol 2019, **29**:e2028.
21. D'Amico F, Mukhopadhyay R, Ovaa H, Mulder MPC: **Targeting TRIM Proteins: A Quest towards Drugging an Emerging Protein Class**. Chembiochem 2021, **22**:2011–2031.
22. Gao B, Wang Y, Xu W, Duan Z, Xiong S: **A 5' extended IFN-stimulating response element is crucial for IFN-gamma-induced tripartite motif 22 expression via interaction with IFN regulatory factor-1**. J Immunol 2010, **185**:2314–2323.
23. Pagani I, Poli G, Vicenzi E: **TRIM22. A Multitasking Antiviral Factor**. Cells 2021, **10**.

24. Turrini F, Marelli S, Kajaste-Rudnitski A, Lusic M, Van Lint C, Das AT, Harwig A, Berkhout B, Vicenzi E: **HIV-1 transcriptional silencing caused by TRIM22 inhibition of Sp1 binding to the viral promoter**. Retrovirology 2015, **12**:104.
25. Di Pietro A, Kajaste-Rudnitski A, Oteiza A, Nicora L, Towers GJ, Mechti N, Vicenzi E: **TRIM22 inhibits influenza A virus infection by targeting the viral nucleoprotein for degradation**. J Virol 2013, **87**:4523–4533.
26. Reddi TS, Merkl PE, Lim SY, Letvin NL, Knipe DM: **Tripartite Motif 22 (TRIM22) protein restricts herpes simplex virus 1 by epigenetic silencing of viral immediate-early genes**. PLoS Pathog 2021, **17**:e1009281.
27. Wang K, Zou C, Wang X, Huang C, Feng T, Pan W, Wu Q, Wang P, Dai J: **Interferon-stimulated TRIM69 interrupts dengue virus replication by ubiquitinating viral nonstructural protein 3**. PLoS Pathog 2018, **14**:e1007287.
28. Manokaran G, Finol E, Wang C, Gunaratne J, Bahl J, Ong EZ, Tan HC, Sessions OM, Ward AM, Gubler DJ, et al: **Dengue subgenomic RNA binds TRIM25 to inhibit interferon expression for epidemiological fitness**. Science 2015, **350**:217–221.
29. Bębnowska D, Niedźwiedzka-Rystwej P: **The Interplay between Autophagy and Virus Pathogenesis-The Significance of Autophagy in Viral Hepatitis and Viral Hemorrhagic Fevers**. Cells 2022, **11**.
30. Li YQ, Hu J, Wang L: **Emerging Roles of the TRIM Family in Autophagy**. Chinese Journal of Biochemistry and Molecular Biology 2021, **37**.
31. Mandell MA, Jain A, Arko-Mensah J, Chauhan S, Kimura T, Dinkins C, Silvestri G, Münch J, Kirchhoff F, Simonsen A, et al: **TRIM proteins regulate autophagy and can target autophagic substrates by direct recognition**. Dev Cell 2014, **30**:394–409.
32. Hu J, Ding X, Tian S, Chu Y, Liu Z, Li Y, Li X, Wang G, Wang L, Wang Z: **TRIM39 deficiency inhibits tumor progression and autophagic flux in colorectal cancer via suppressing the activity of Rab7**. Cell Death Dis 2021, **12**:391.
33. Pan X, Chen Y, Shen Y, Tantai J: **Knockdown of TRIM65 inhibits autophagy and cisplatin resistance in A549/DDP cells by regulating miR-138-5p/ATG7**. *Cell Death Dis* 2019, **10**:429.
34. Xiao F, Ouyang B, Zou J, Yang Y, Yi L, Yan H: **Trim14 promotes autophagy and chemotherapy resistance of gastric cancer cells by regulating AMPK/mTOR pathway**. Drug Dev Res 2020, **81**:544–550.
35. Wu W, Luo X, Ren M: **Clearance or Hijack: Universal Interplay Mechanisms Between Viruses and Host Autophagy From Plants to Animals**. Front Cell Infect Microbiol 2021, **11**:786348.
36. Paul P, Münz C: **Autophagy and Mammalian Viruses: Roles in Immune Response, Viral Replication, and Beyond**. Adv Virus Res 2016, **95**:149–195.
37. Sparrer KMJ, Gack MU: **TRIM proteins: New players in virus-induced autophagy**. PLoS Pathog 2018, **14**:e1006787.
38. Stremlau M, Owens CM, Perron MJ, Kiessling M, Autissier P, Sodroski J: **The cytoplasmic body component TRIM5alpha restricts HIV-1 infection in Old World monkeys**. Nature 2004, **427**:848–853.

39. Jena KK, Kolapalli SP, Mehto S, Nath P, Das B, Sahoo PK, Ahad A, Syed GH, Raghav SK, Senapati S, et al: **TRIM16 controls assembly and degradation of protein aggregates by modulating the p62-NRF2 axis and autophagy**. Embo j 2018, **37**.
40. Sparrer KMJ, Gableske S, Zurenski MA, Parker ZM, Full F, Baumgart GJ, Kato J, Pacheco-Rodriguez G, Liang C, Pornillos O, et al: **TRIM23 mediates virus-induced autophagy via activation of TBK1**. Nat Microbiol 2017, **2**:1543–1557.
41. Mariño G, Niso-Santano M, Baehrecke EH, Kroemer G: **Self-consumption: the interplay of autophagy and apoptosis**. Nat Rev Mol Cell Biol 2014, **15**:81–94.

Figures

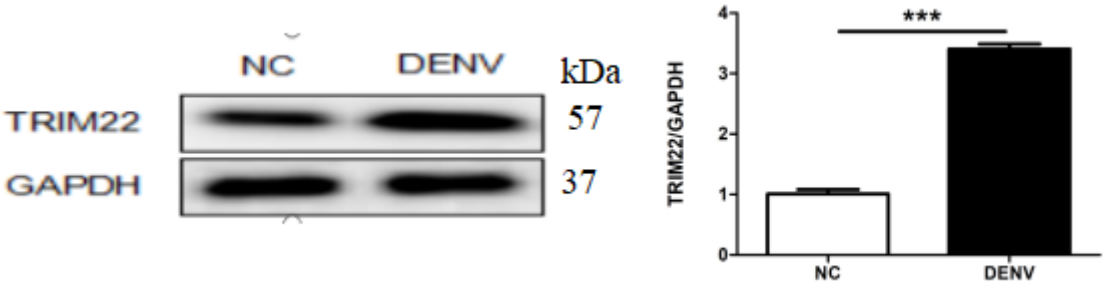

Figure 1

TRIM22 protein expression in HUVECs infected with DENV-2.

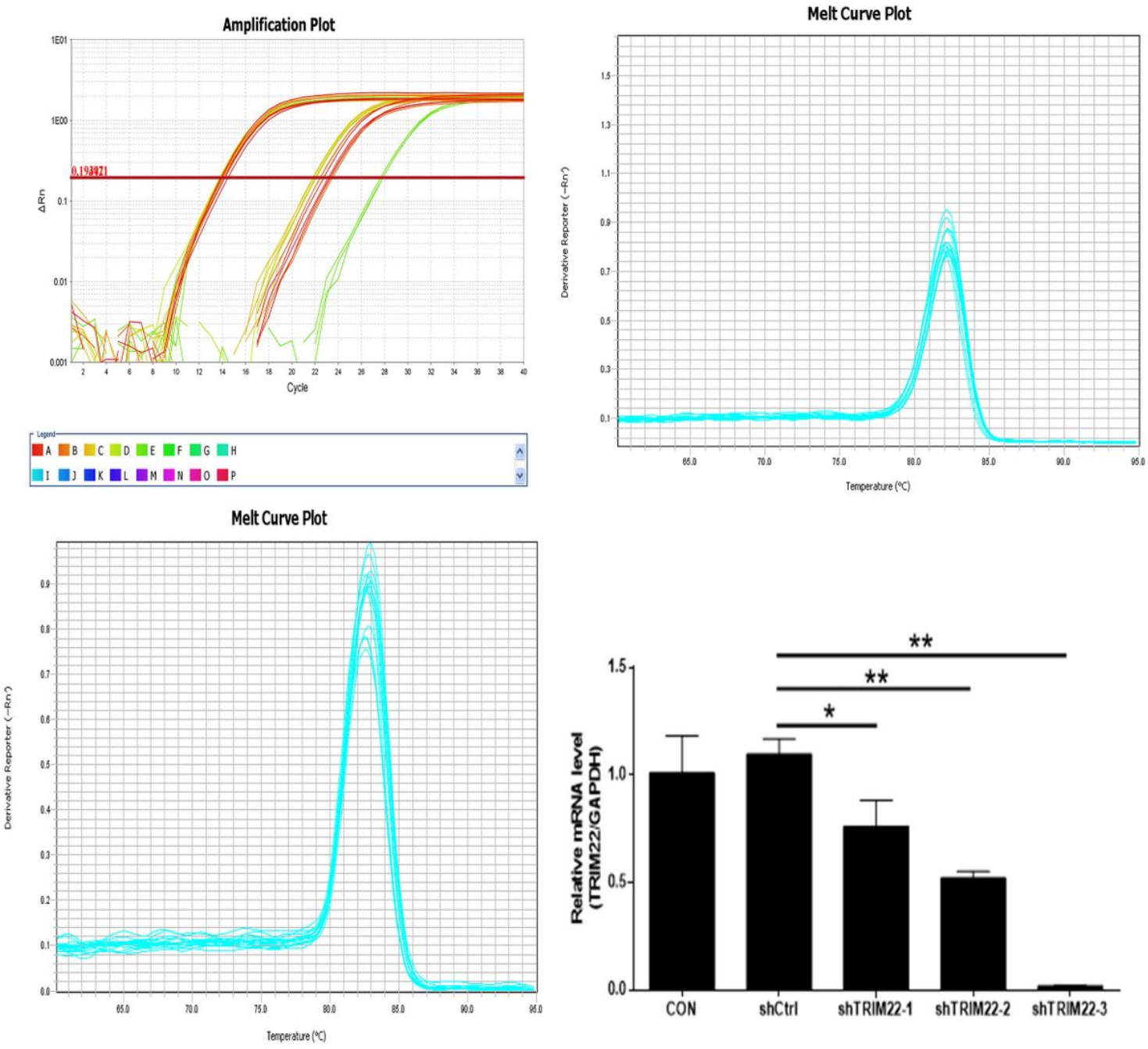

Figure 2

Screening of effective interference targets by qRT-PCR. shTRIM22-1, shTRIM22-2, and shTRIM22-3 were used to target TRIM22.

Figure 3

Knockdown efficiency detection. **A** The TRIM22 expression level after knockdown as detected by qRT-PCR and **B** TRIM22 protein after *TRIM22* gene knockdown as detected by western blot analysis.

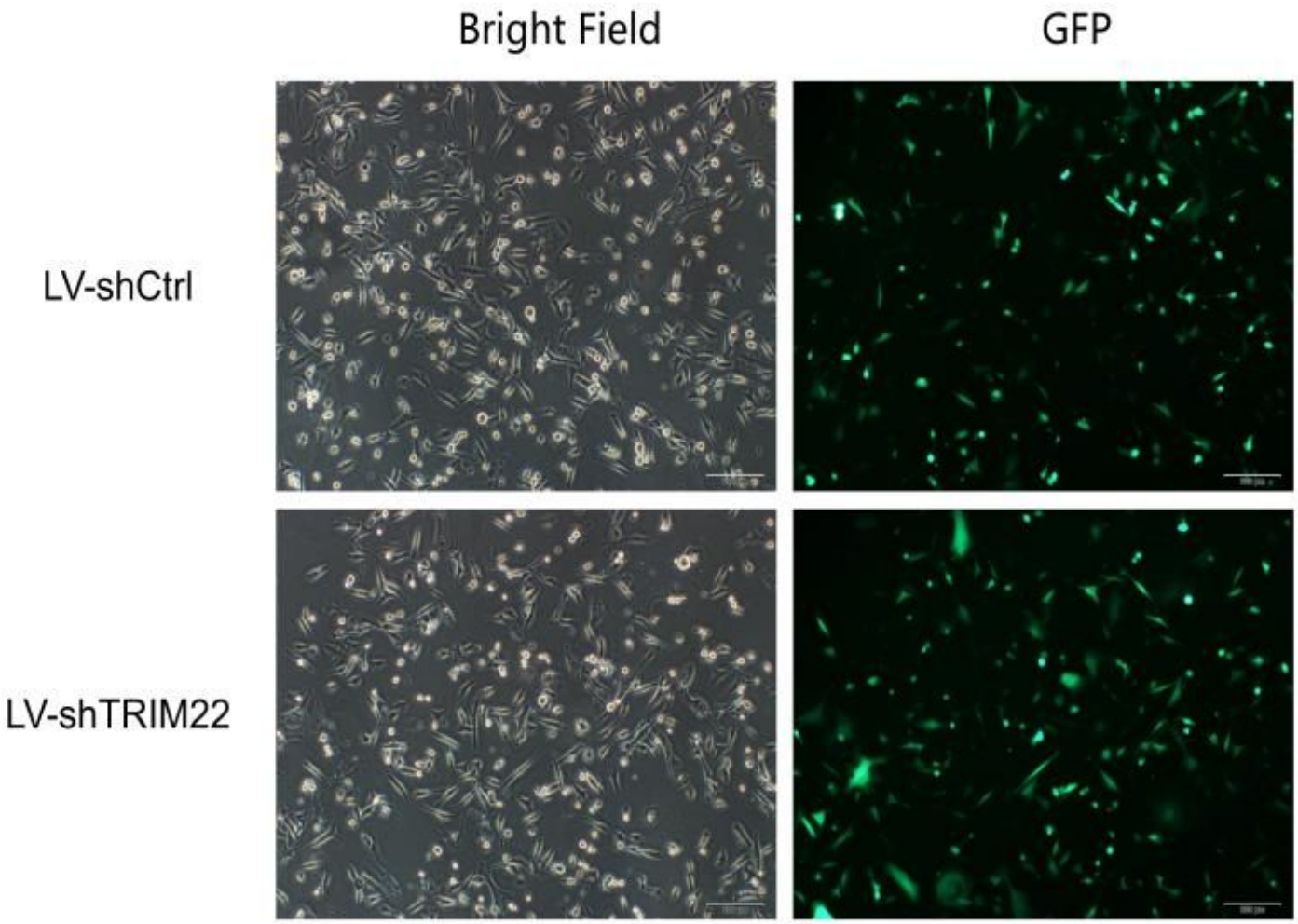

Figure 4

Lentivirus infection of HUVEC (200×).

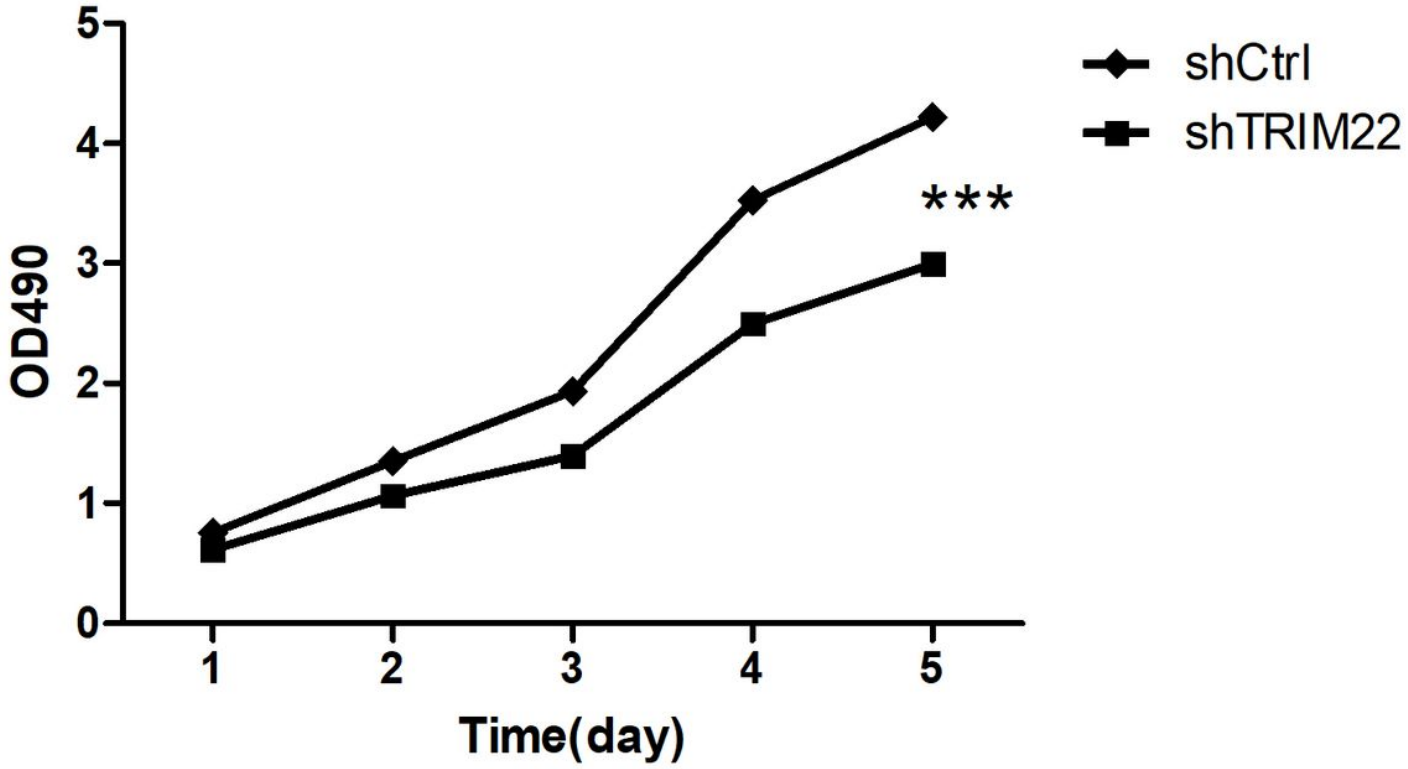

Figure 5

The effect of shTRIM22 on cell proliferation as detected by CCK-8 assay.

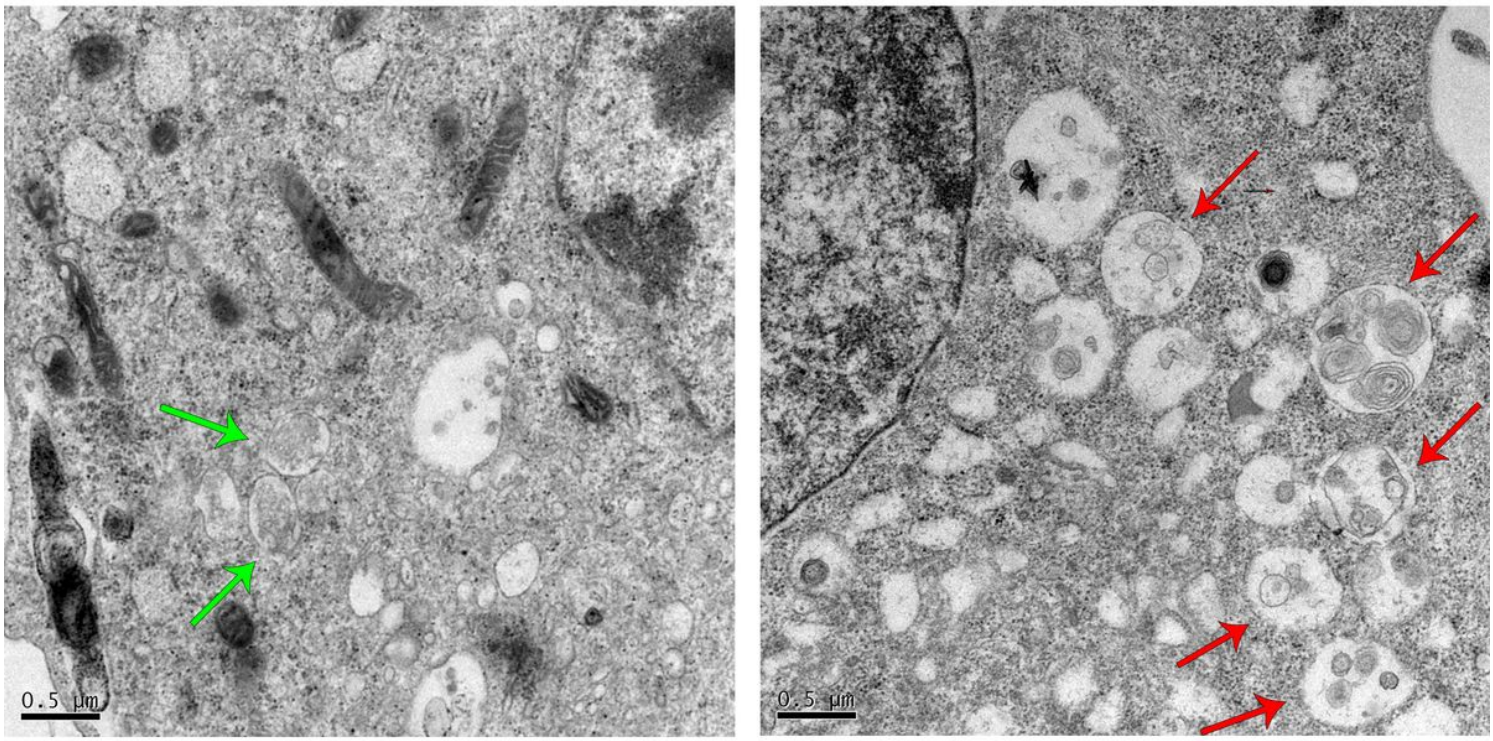

Figure 6

The ultrastructure of HUVEC autophagy after TRIM22 knockdown observed by TEM. *Green arrow*: autophagosome, *red arrow*: autolysosome.

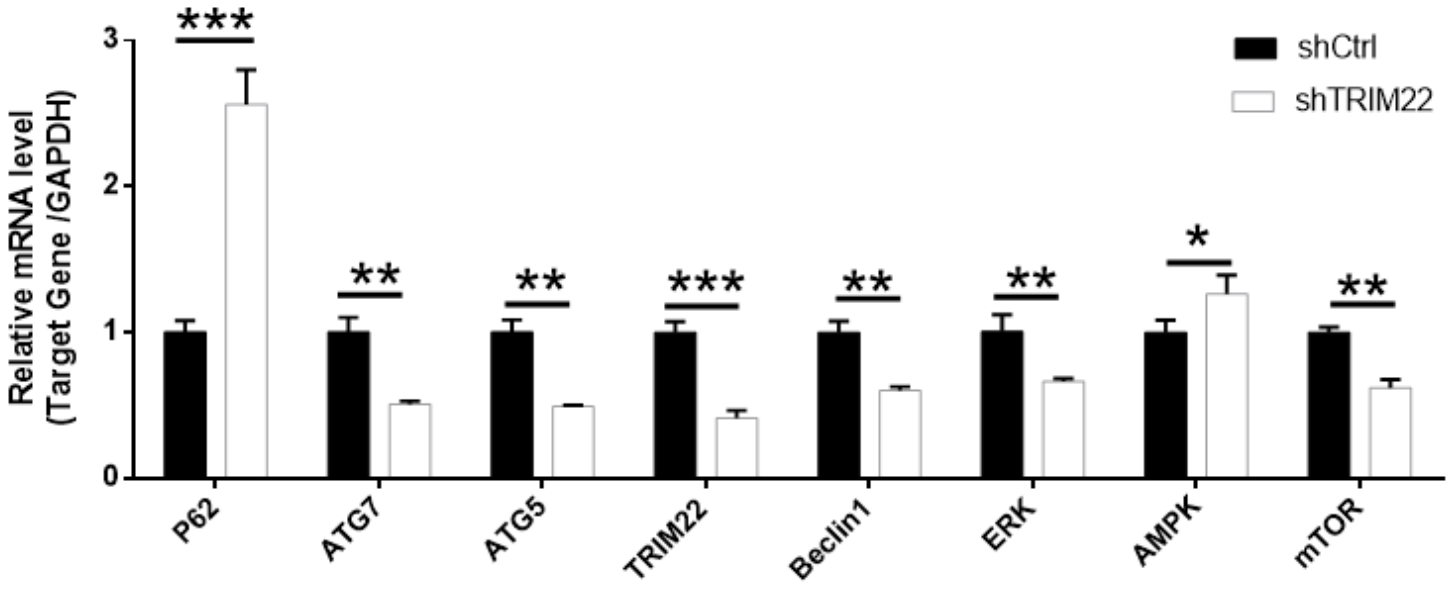

Figure 7

Expression of HUVEC autophagy and AMPK pathway-related genes after TRIM22 knockdown.

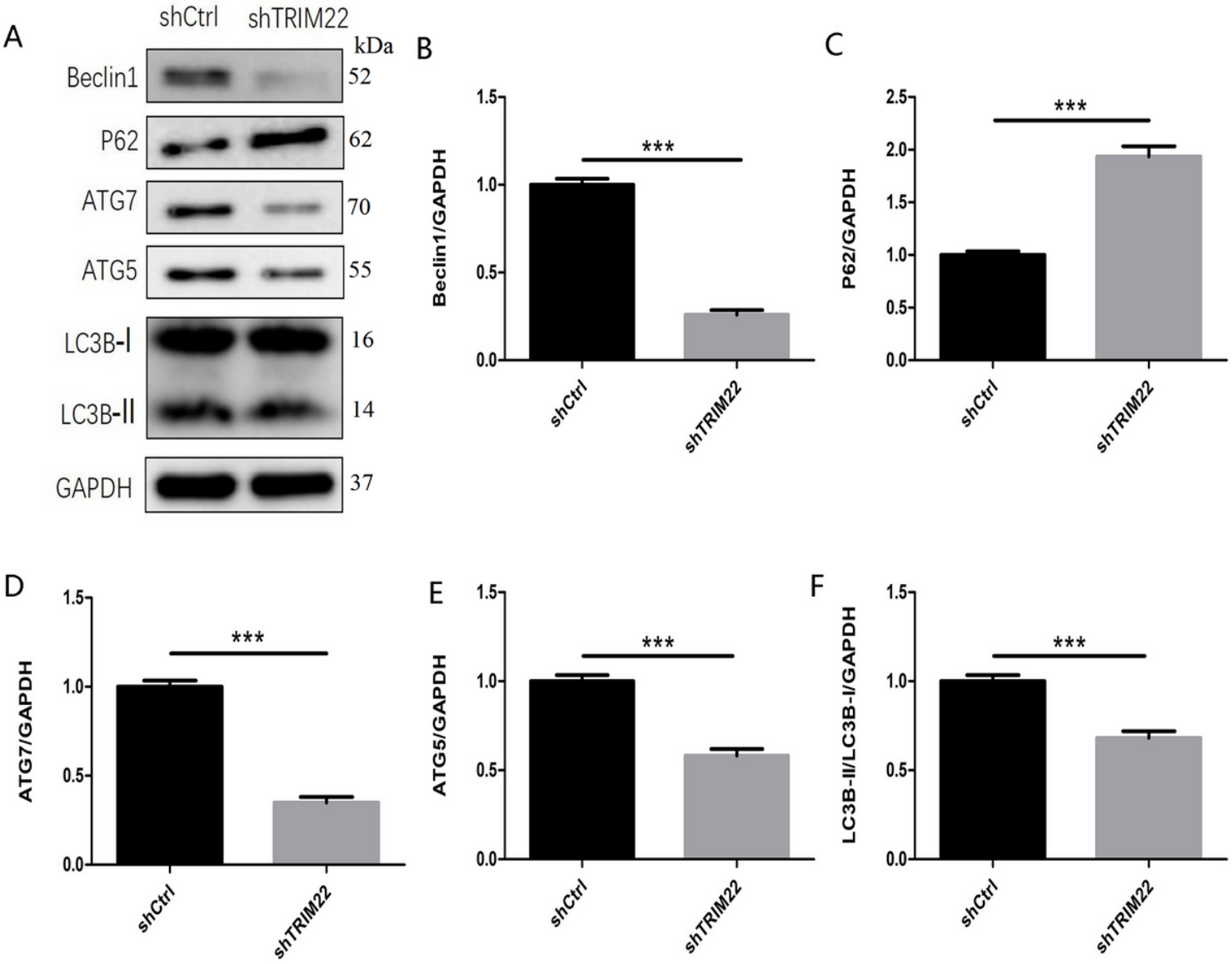

Figure 8

Expression of HUVEC autophagy-related proteins after TRIM22 knockdown. **A** Effect of TRIM22 knockdown on the expression of HUVEC autophagy-related proteins as detected by Western blot analysis, **B** Beclin1 protein expression levels, **C** P62 protein expression levels, **D** ATG7 protein expression levels, **E** ATG5 protein expression levels, and **F** LC3II protein expression levels.

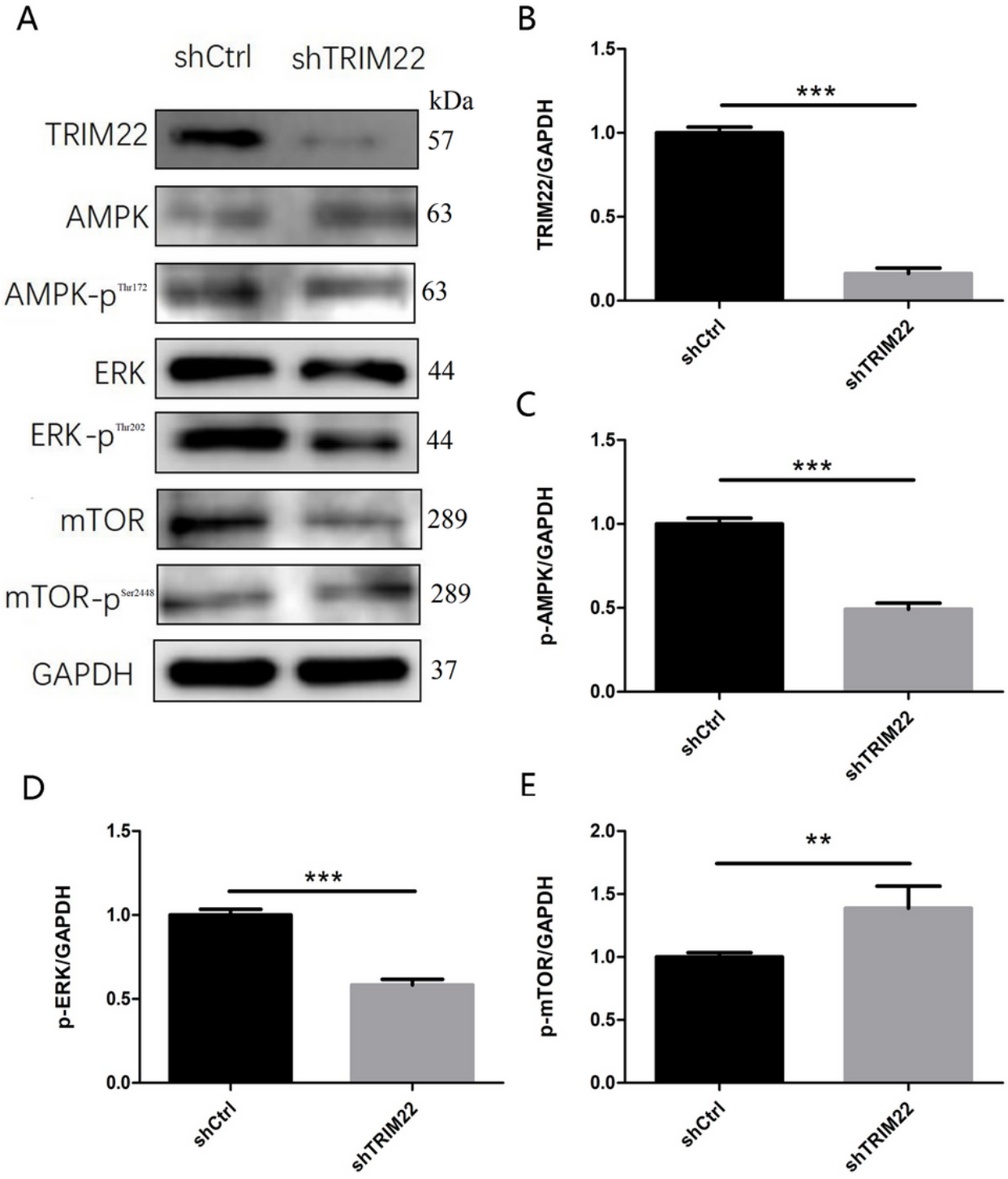

Figure 9

Expression of AMPK pathway-related proteins in HUVECs after TRIM22 knockdown. **A** Effects of TRIM22 knockdown on AMPK pathway-related protein expression in HUVECs as detected by western blot analysis, **B** TRIM22 protein expression levels, **C** p-AMPK protein expression levels, **D** p-ERK protein expression levels, and **E** p-mTOR protein expression levels.

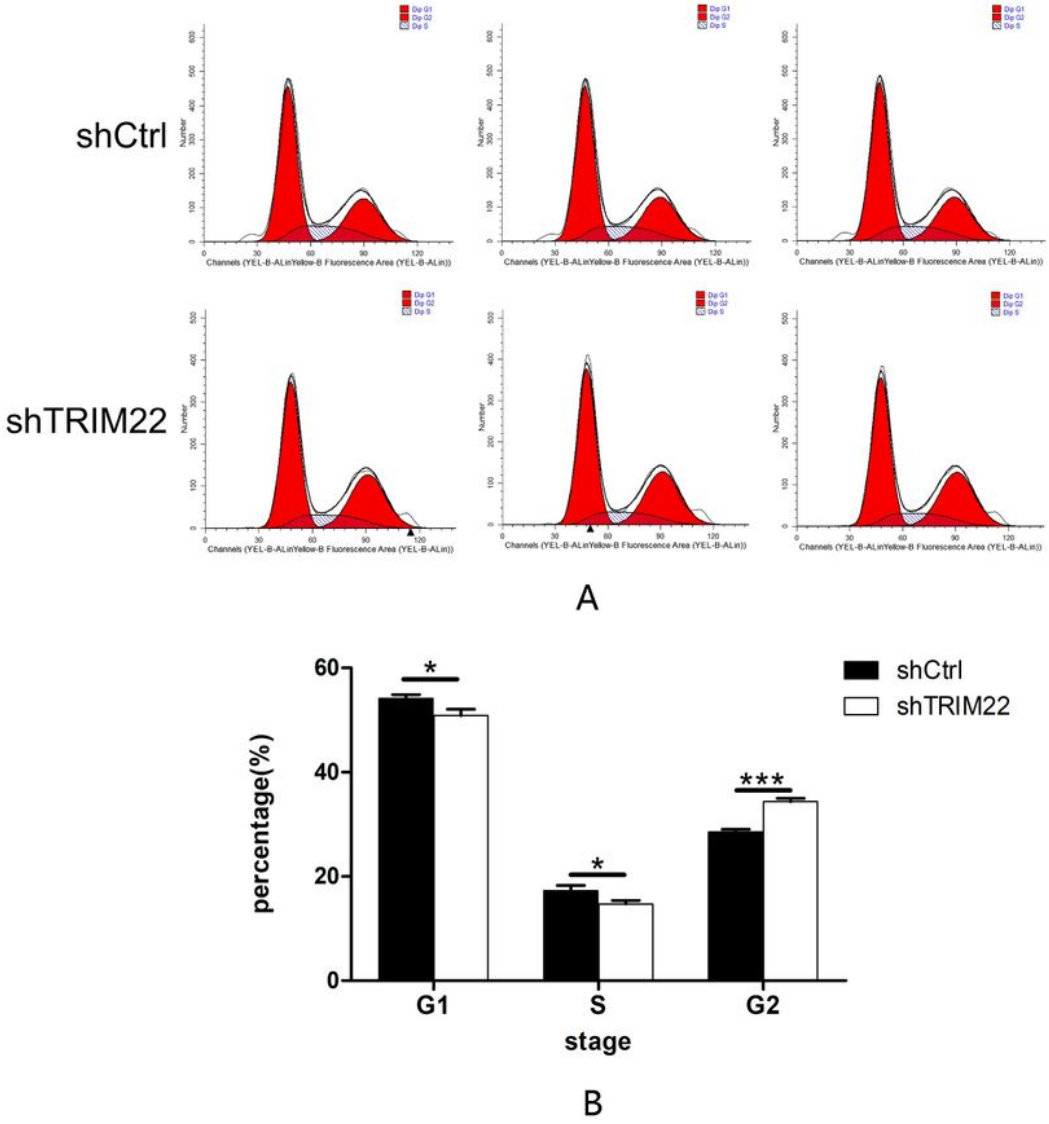

Figure 10

Effect of TRIM22 knockdown on the cell cycle following DENV-2 infection of HUVECs. **A** DNA of HUVECs after TRIM22 knockdown, the abscissa is the fluorescence intensity of PI, which represents the DNA content of the cells, and the ordinate is the number of cells; **B** histogram analysis of each phase of the cell cycle.

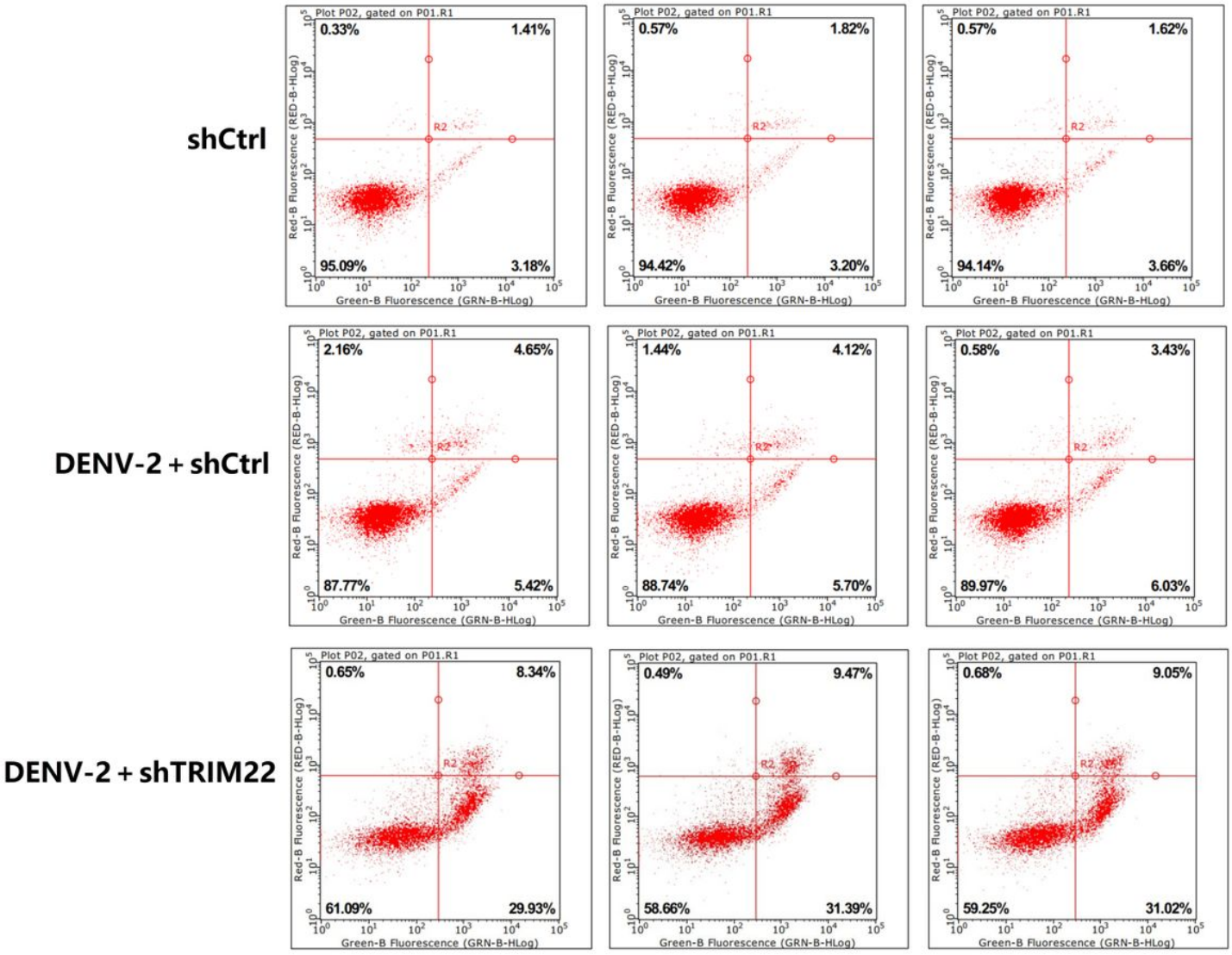

Figure 11

Effect of TRIM22 knockdown on HUVEC apoptosis following DENV-2 infection. *ShCtrl* negative control group, *DENV-2 + shCtrl* negative control group for DENV-2 infection, *DENV-2 + vshTRIM22* DENV-2 infected HUVECs with TRIM22 knockdown.

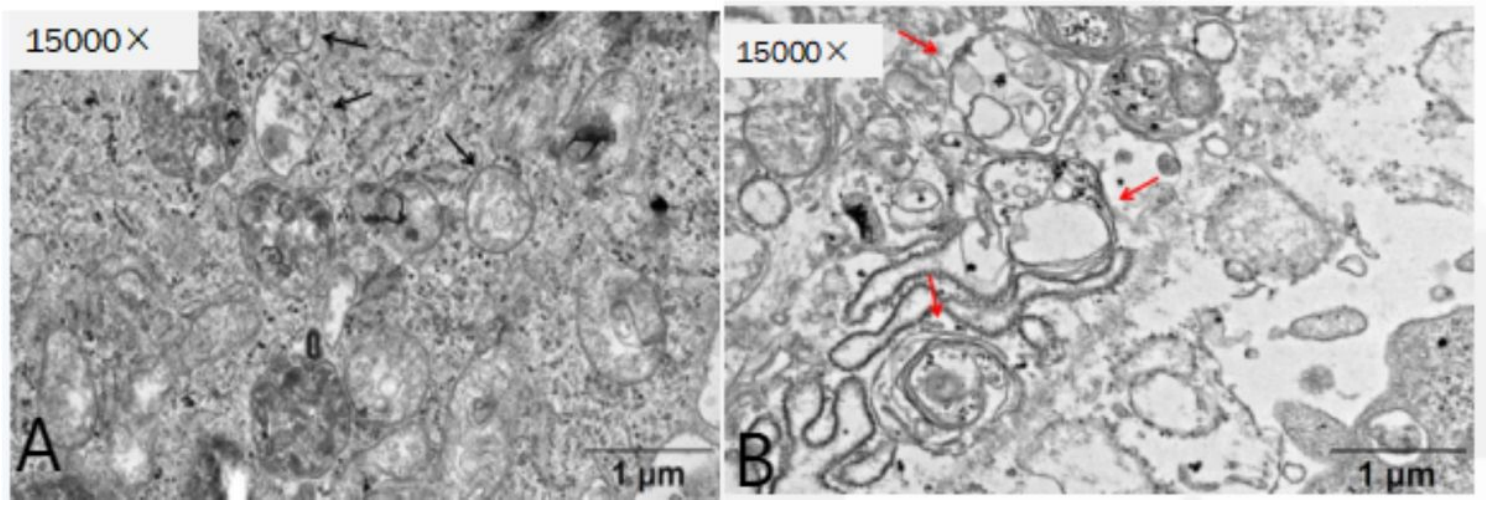

Figure 12

The ultrastructure of DENV-2-infected HUVECs after TRIM22 knockdown as observed by TEM. **A** Control group infected with DENV-2; **B** DENV-2-infected HUVEC group with TRIM22 knockdown. *Black arrow* autophagosome; *red arrow* autolysosome.

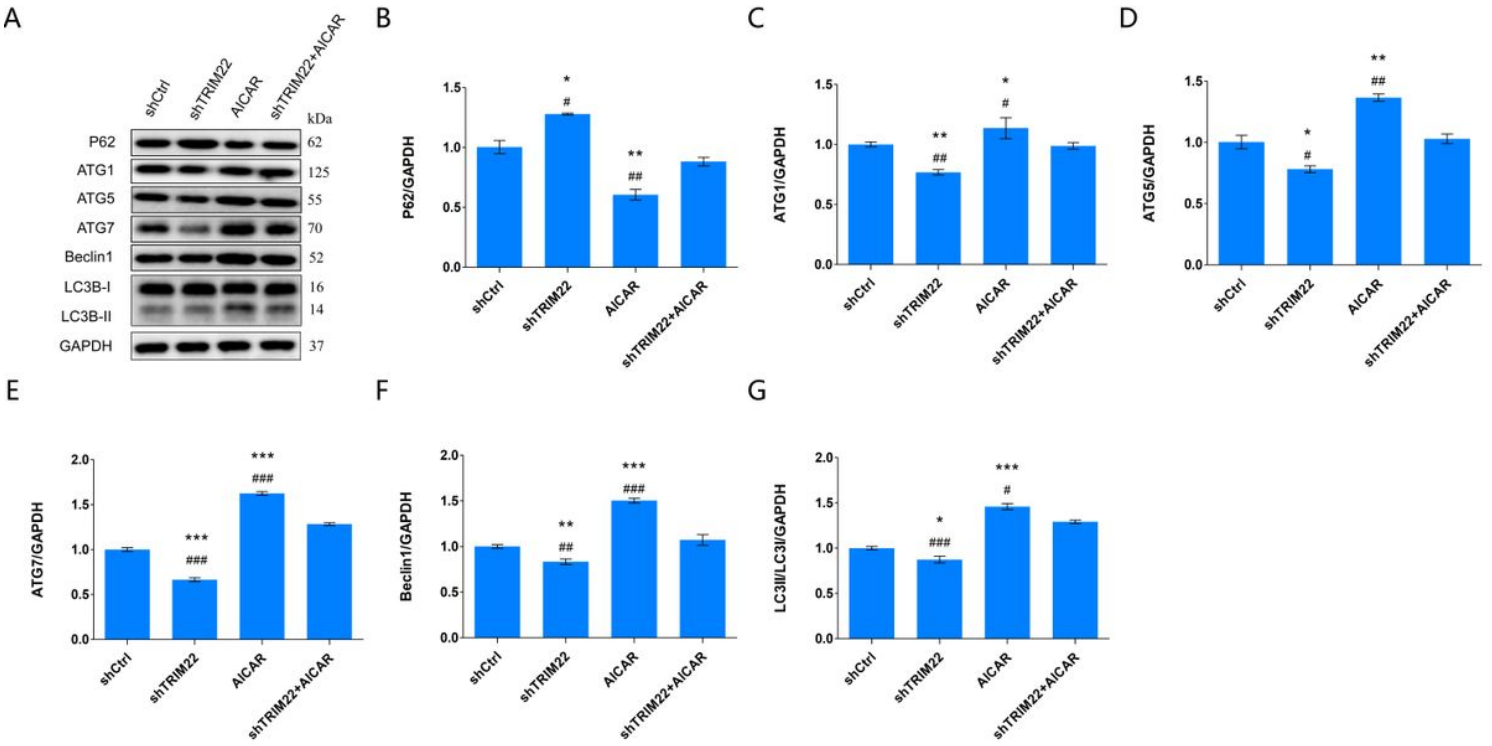

Figure 13

Effect of TRIM22 knockdown on autophagy-related factors in HUVECs following DENV-2 infection. *shCtrl group*: DENV-2 + shCtrl group; *shTRIM22 group*: DENV-2 + shTRIM22 group; *AICAR group*: DENV-2 + shCtrl + AICAR group; *shTRIM22 + AICAR group*: DENV-2 + TRIM22 + AICAR group. *represents comparison with the shCtrl group; $^{*}p < 0.05$, $^{**}p < 0.01$, and $^{***}p < 0.001$. #represents comparison with the shTRIM22 + AICAR group; $^{\#}p < 0.05$, $^{\#\#}p < 0.01$, and $^{\#\#\#}p < 0.001$. **A** Effect of TRIM22 knockdown on the

expression of DENV-2-induced HUVEC autophagy-related proteins detected by western blot analysis; **B** P62 protein expression levels; **C** ATG1 protein expression levels; **D** ATG5 protein expression levels; **E** ATG7 protein expression levels; **F** Beclin1 protein expression levels; and **G** LC3II/LC3I protein expression levels.

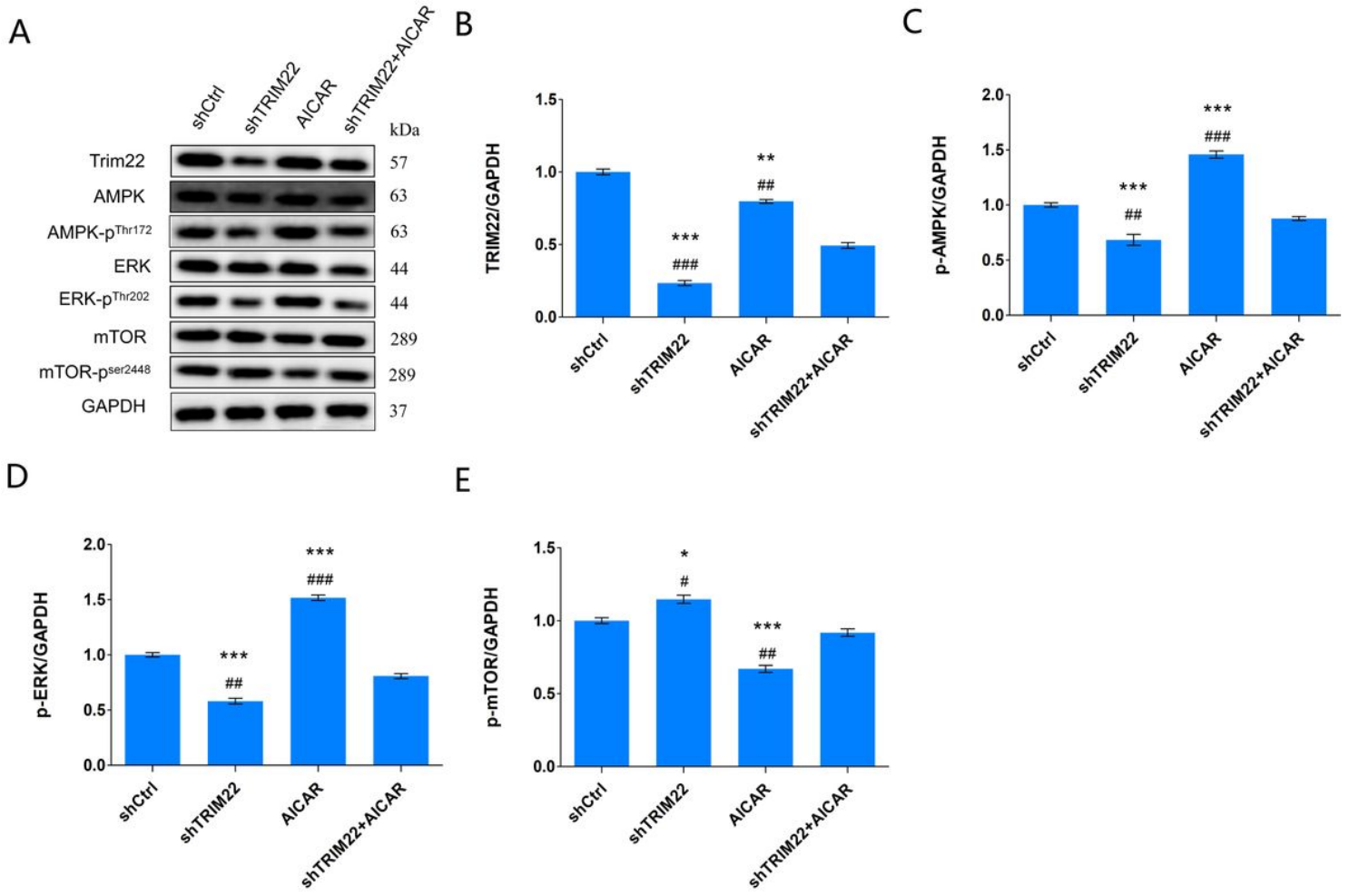

Figure 14

Effects of TRIM22 knockdown on the expression of AMPK/ERK/mTOR pathway-related proteins in HUVECs infected with DENV-2. *represents comparison with the shCtrl group; $^{*}p < 0.05$, $^{**}p < 0.01$, and $^{***}p < 0.001$. #represents comparison with the shTRIM22 + AICAR group; $^{\#}p < 0.05$, $^{\#\#}p < 0.01$, and $^{\#\#\#}p < 0.001$. **A** Effects of TRIM22 knockdown on the expression of AMPK/ERK/mTOR pathway-related proteins in HUVECs infected with DENV-2 as detected by western blot analysis; **B** TRIM22 protein expression levels; **C** p-AMPK protein expression levels; **D** p-ERK protein expression levels; and **E** p-mTOR protein expression levels.

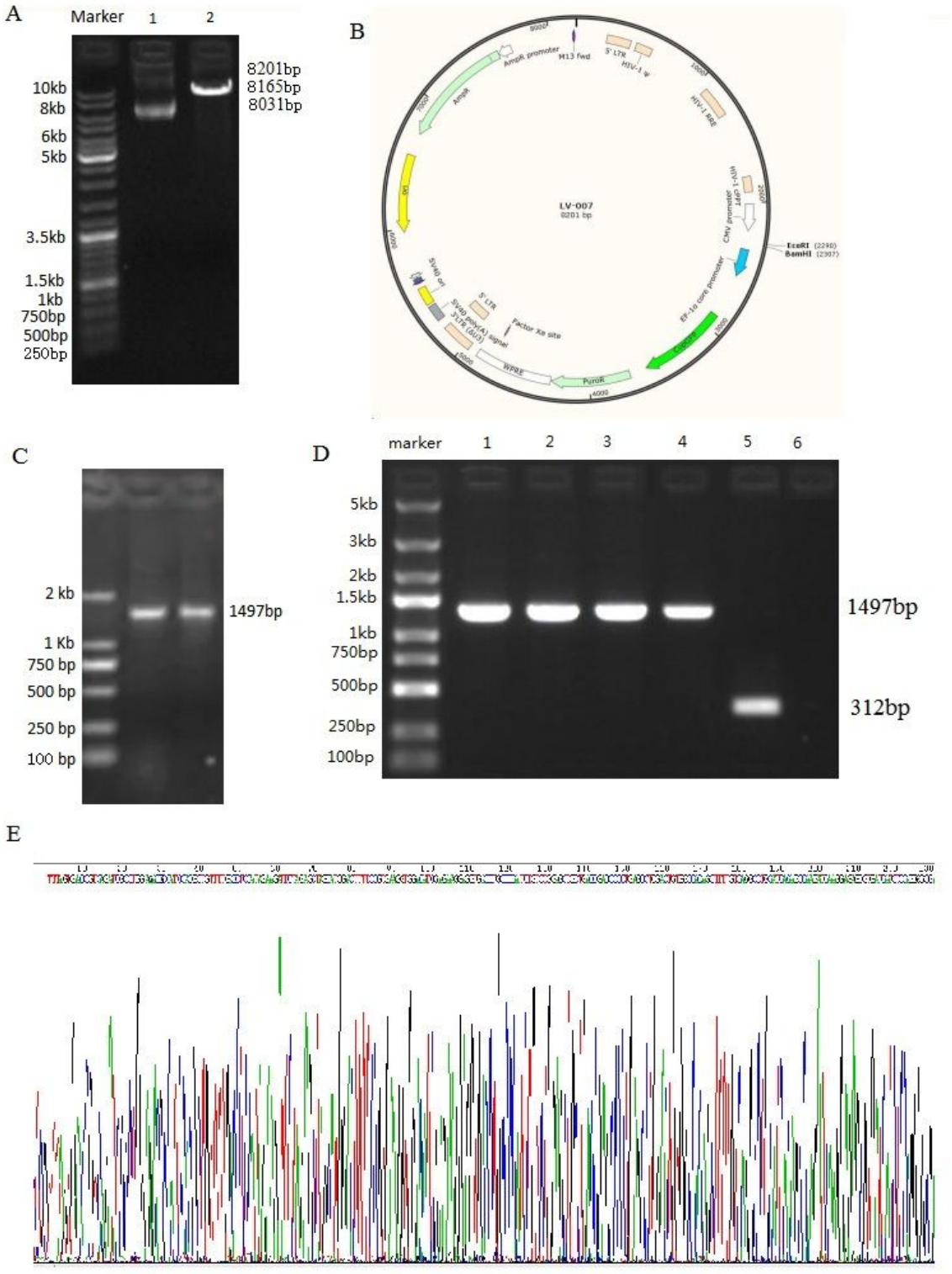

Figure 15

Establishment of a TRIM22 overexpression plasmid. **A** Results of agarose gel electrophoresis of the restriction enzyme-digested vector; *1* LV-007 Vector linearized by Nhe I and Age I double digestion, *2* LV-007 Vector (vector plasmid without digestion); **B** Lv-007 vector map. Component order: CMV-MCS-EF1-copGFP-T2A-puromycin; fluorescent tags: copGFP; clone sites: Age I and BamHI. **C** Electrophoresis of the TRIM22 PCR products. A specific band at ~1,497 bp, which was consistent with the expected size, was

noted. **D** *1–4* positive transformants of the TRIM22 overexpression plasmid; *5* negative control (no-load self-connecting control group). The negative control was used to show no false positives in the amplification process using empty vectors without the target gene as templates. The PCR product size of the negative transformant was 312 bp. *6* Negative control (ddH_2O). False positives result from the contamination of external nucleic acid in the exclusion system.

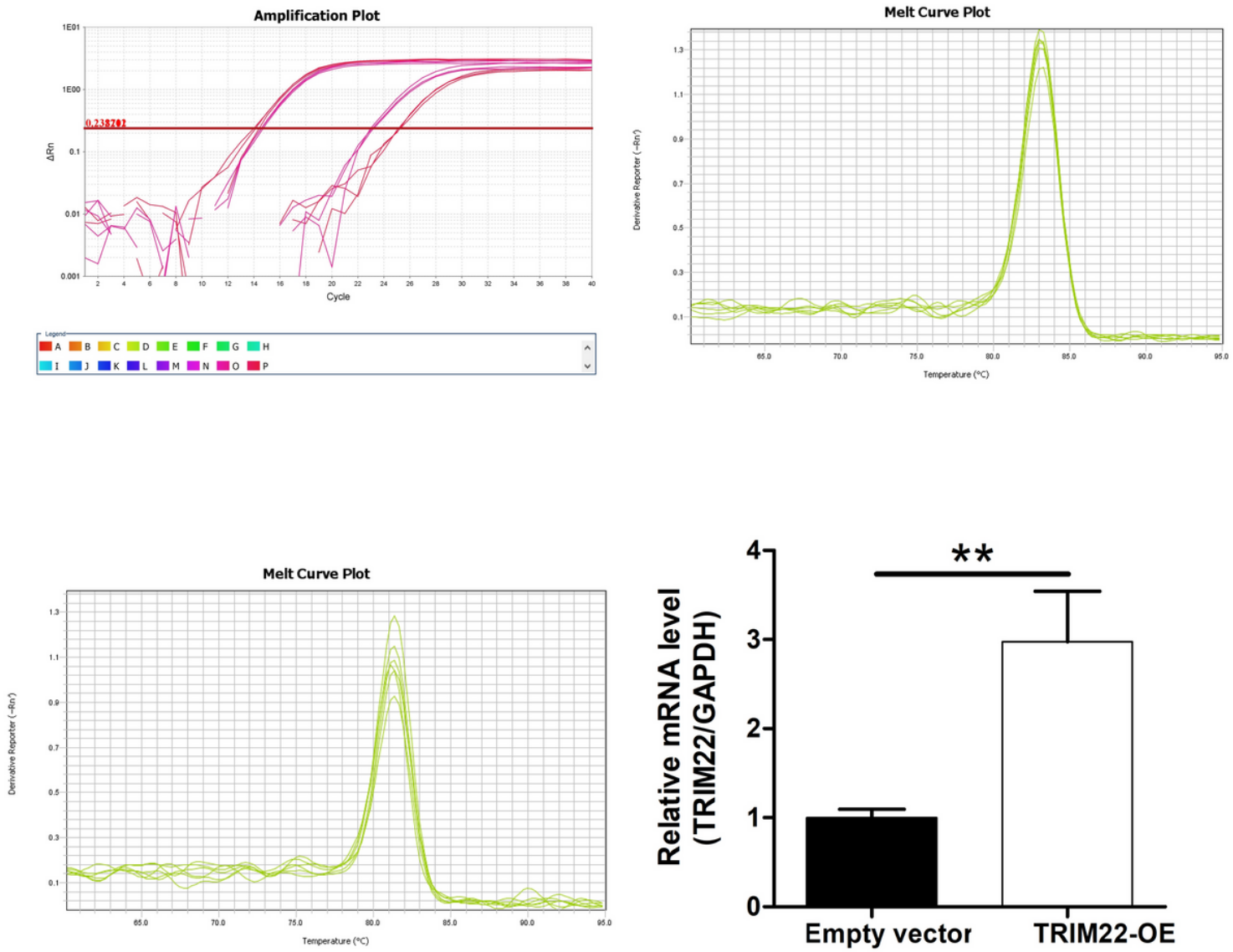

Figure 16

TRIM22 overexpression efficiency in HUVECs detected by RT-qPCR.

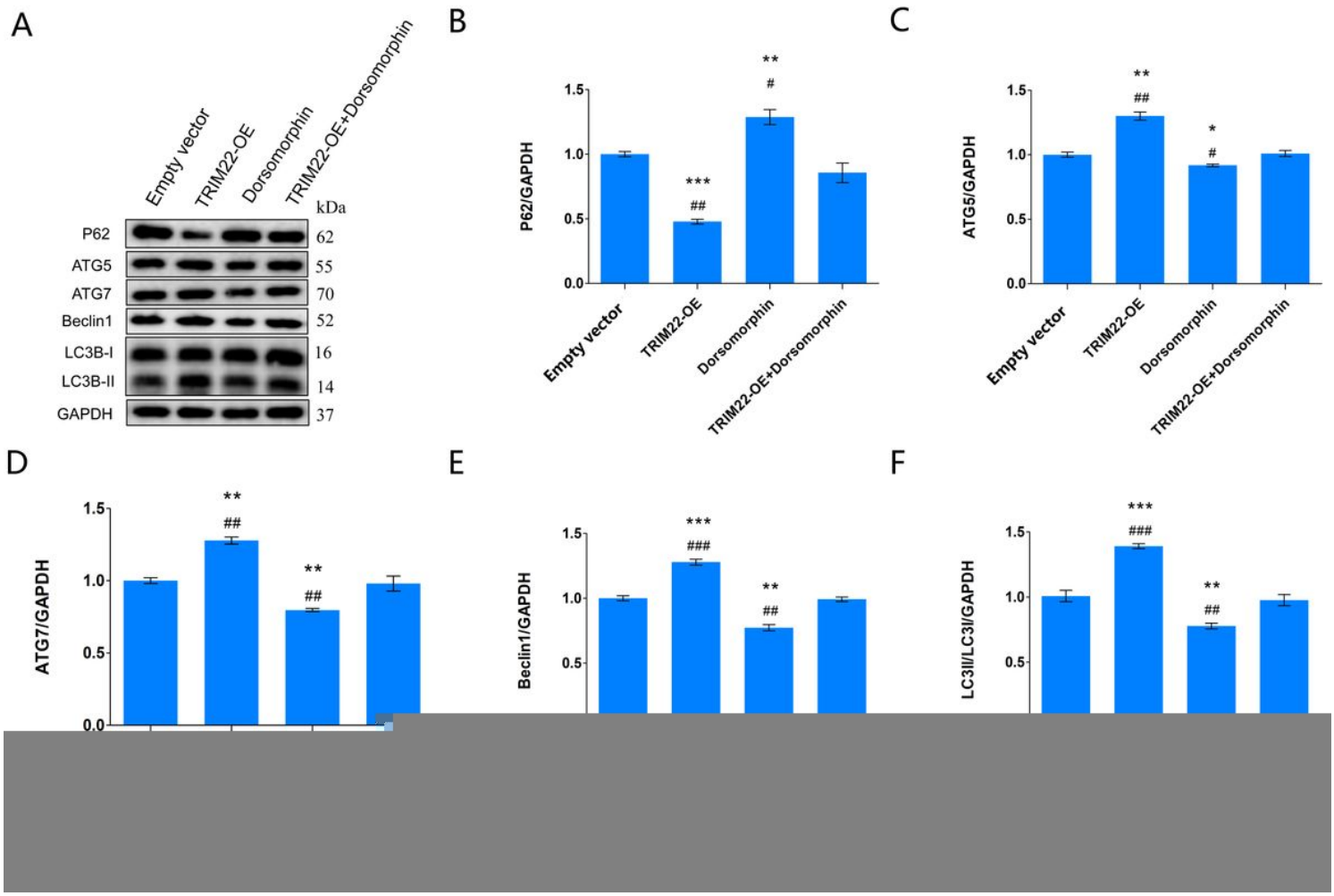

Figure 17

Effect of TRIM22 overexpression on HUVEC autophagy-related factors infected with DENV-2. *TRIM22-OE*: TRIM22 overexpression group; *Dorsomorphin*: AMPK inhibitor. *Empty vector*: DENV-2 + Empty vector group; *TRIM22-OE*: DENV-2 + TRIM22-OE group; *3-MA*: DENV-2 + Empty vector + Dorsomorphin; *Dorsomorphin + TRIM22-OE*: DENV-2 + TRIM22-0E + Dorsomorphin group. *represents comparison with the Empty vector group; $^{*}p < 0.05$, $^{**}p < 0.01$, and $^{***}p < 0.001$. #represents comparison with the TRIM22-OE + Dorsomorphin group; $^{\#}p < 0.05$, $^{\#\#}p < 0.01$, and $^{\#\#\#}p < 0.001$. **A** Effects of TRIM22 overexpression on autophagy-related factors in DENV-2-infected HUVECs as detected by western blot analysis. **B** P62 protein expression levels; **C** ATG5 protein expression levels; **D** ATG7 protein expression levels; **E** Beclin1 protein expression levels; and **F** LC3II/LC3I protein expression levels.

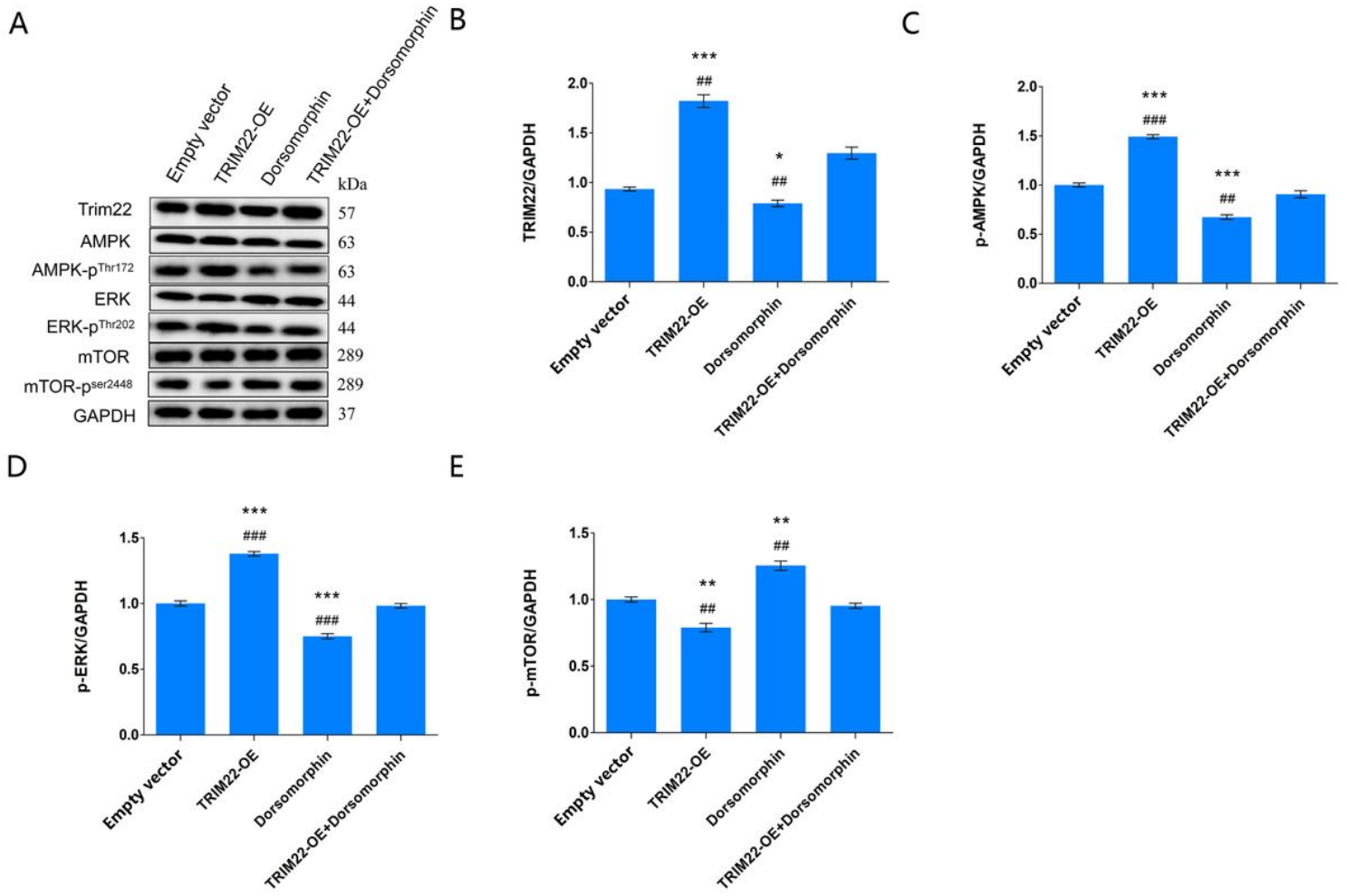

Figure 18

Effects of TRIM22 overexpression on AMPK/ERK/mTOR signaling pathway-related proteins of HUVECs infected with DENV-2. *represents comparison with the Empty vector group; $^{*}p < 0.05$, $^{**}p < 0.01$, and $^{***}p < 0.001$. #represents comparison with the TRIM22-OE + Dorsomorphin group, $^{\#}p < 0.05$, $^{\#\#}p < 0.01$, $^{\#\#\#}p < 0.001$. **A** Effects of TRIM22 overexpression on AMPK/ERK/mTOR signaling pathway-related proteins of HUVECs infected with DENV-2 as detected by western blot analysis; **B** TRIM22 protein expression levels; **C** p-AMP protein expression levels; **D** p-ERK protein expression levels; and **E** p-mTOR expression levels.